7

Overview of analytic methods for multivariate GFs

We now return to the problem at the heart of this book: asymptotically approximating the coefficients of a convergent Laurent series expansion $F(\boldsymbol{z}) = \sum_{\boldsymbol{r} \in \mathbb{Z}^d} a_{\boldsymbol{r}} \boldsymbol{z}^{\boldsymbol{r}}$ through the Cauchy integral representation

$$a_{\boldsymbol{r}} = \left(\frac{1}{2\pi i}\right)^d \int_T \boldsymbol{z}^{-\boldsymbol{r}-\mathbf{1}} F(\boldsymbol{z})\, d\boldsymbol{z}\,, \tag{7.1}$$

for a suitable domain of integration T. We accomplish this by deforming T and using residue computations to reduce the Cauchy integral into a finite sum of local integrals that can be asymptotically approximated using the results of Chapter 5. When this approach succeeds, which it does in *generic* situations, it provides asymptotic formulae of the form

$$a_{\boldsymbol{r}} \approx \sum_{\boldsymbol{w} \in \mathrm{critical}(\hat{\boldsymbol{r}})} n_{\boldsymbol{w}} \Phi_{\boldsymbol{w}}(\boldsymbol{r})\,, \tag{7.2}$$

where the sum is over a finite set of certain *critical points* $\boldsymbol{w}$, each $\Phi_{\boldsymbol{w}}$ is an asymptotic series that can be computed to any desired accuracy algorithmically, and the coefficients $n_{\boldsymbol{w}}$ are integers that may or may not be easy to compute.

This textbook is designed so that combinatorialists can find easy-to-apply results with hypotheses and conclusions that are comprehensible with a minimum of cross-referencing to lengthy definitions, while readers with topological background can see the larger framework behind the results using advanced methods, such as those described in Chapters 4–6 and the appendices. In order to achieve this goal, the current chapter gives an overview of our approach and its relationship to the higher-level theories we draw on. Chapter 8 takes a computational view of the same material, giving explicit descriptions of how to compute the quantities appearing in the analysis using a computer algebra system. This material out of the way, Chapters 9–11 give our asymptotic

https://doi.org/10.1017/9781108874144.012 Published online by Cambridge University Press

results for families of generating functions with increasingly complicated singular behavior, together covering most known examples of rational generating functions in the combinatorial literature. Chapter 12 then gives a large variety of examples and applications before Chapter 13 describes further extensions.

In order to guide intuition and introduce the high-level constructions to be used in later chapters of the book, the current chapter begins by sketching the analysis on some examples, showing how the computations in the simplest case are a straightforward generalization of the univariate methods from Part I, describing the limits of these methods, and illustrating why we require more advanced techniques for our strongest results. After this we introduce the algebraic and topological constructions necessary for our work, and prove the theoretical results underpinning later chapters.

The computation of asymptotics is considerably simpler, and easier to explain, when the set of singularities $\mathcal{V}$ of F is *smooth* (meaning it is a manifold, at least near points dictating asymptotics). Before going into technical details, we illustrate the smooth case through extended examples in Section 7.1. Readers who want to understand the method but not the details can quit after the examples and skip to Chapters 8 and 9. In Section 7.2 we describe the theory when $\mathcal{V}$ is smooth, allowing readers to understand the smooth point formulae of Chapter 9 without the greater overhead of stratified Morse theory.

Section 7.3 gives a parallel treatment of everything in the previous sections, without the assumption that $\mathcal{V}$ is smooth. This involves the introduction of stratified Morse theory to explain the corresponding notions of critical points and *quasi-local cycles* for non-smooth varieties. The quasi-local cycles are defined in terms of the *tangential cycles* γ_j and homology generators β_j for the *normal link* at $\boldsymbol{z}_j$. Section 7.4 discusses the types of singular geometry that arise frequently in combinatorial applications.

The results of (stratified) Morse theory describe the topology of a surface using a *height function* mapping the surface to the real numbers. In classical Morse theory this height function is almost always assumed to be proper, meaning the set of points with heights in a closed interval forms a compact set. Unfortunately, we work in situations where the height function is usually *non-proper*. To get around this difficulty, Section 7.5 introduces the concept of *critical points at infinity* (CPAI) and *critical values at infinity* (CVAI), which help characterize when the results of Morse theory we need apply without an assumption of a proper height function. A fundamental lemma is stated concerning the existence of certain deformations, provided there are no critical values at infinity, and its proof is cited from the literature. This lemma is then used to prove the theorems previously stated in the chapter.

https://doi.org/10.1017/9781108874144.012 Published online by Cambridge University Press

Notational conventions

For the rest of this book we use the following notational conventions. Bold quantities are reserved for vectors, such as $\boldsymbol{z} = (z_1, \ldots, z_d)$, and we define $\boldsymbol{z}^\circ := (z_1, \ldots, z_{d-1})$. The d-variate function $F(\boldsymbol{z})$ is a quotient of coprime polynomials $P(\boldsymbol{z})/Q(\boldsymbol{z})$, with the denominator Q vanishing on the ***singular variety*** $\mathcal{V} = \mathcal{V}_Q = \{\boldsymbol{z} \in \mathbb{C}^d : Q(\boldsymbol{z}) = 0\}$. We fix a component B of the complement of $\texttt{amoeba}(Q)$ and consider the Laurent series expansion $F(\boldsymbol{z}) = \sum_{\boldsymbol{r}\in\mathbb{Z}^d} a_{\boldsymbol{r}} \boldsymbol{z}^{\boldsymbol{r}}$ that converges on $\mathcal{D} = \text{Relog}^{-1}(B)$. As in previous chapters, for $\boldsymbol{w} \in \mathbb{C}_*^d$ we use the notation $\mathbf{T}(\boldsymbol{w})$ for the torus $\mathbf{T}(\boldsymbol{w}) = \{\boldsymbol{z} \in \mathbb{C}^d : |z_j| = |w_j| \text{ for all } j\}$. The simplest and most common case, of a convergent power series expansion, occurs when B is the component containing points of the form $(-N, \ldots, -N)$ for N sufficiently large, so that $\mathcal{D}$ is a neighborhood of the origin.

Remark 7.1. Although we mainly study rational generating functions, most of our results also hold for meromorphic functions. We point out as we go which major results still hold for meromorphic functions, and the small ways in which they differ from the rational case.

Given $\boldsymbol{r} \in \mathbb{Z}^d$ the d-form $\omega = \boldsymbol{z}^{-\boldsymbol{r}-\mathbf{1}} F(\boldsymbol{z}) d\boldsymbol{z}$ is the integrand of the Cauchy integral (7.1), with domain of analyticity $\mathcal{M} = \mathbb{C}_*^d \setminus \mathcal{V}$. Unless otherwise stated, we write $|\boldsymbol{r}|$ for the ℓ^1-norm $|\boldsymbol{r}| = \sum_{j=1}^d |r_j|$ and as above define the normalized vector $\hat{\boldsymbol{r}} = \boldsymbol{r}/|\boldsymbol{r}|$. We seek to compute asymptotics for the series coefficients $a_{\boldsymbol{r}}$ as $\boldsymbol{r} \to \infty$ with $\hat{\boldsymbol{r}}$ varying over a compact set, typically around some fixed direction.

7.1 Some illustrative examples

Example 7.2 (Binomial Coefficients)**.** We start with perhaps the simplest nontrivial bivariate rational function for our purposes: $F(x, y) = 1/Q(x, y)$ with $Q(x, y) = 1 - x - y$. The amoeba of Q is pictured in Figure 7.1 (see Chapter 8 for methods to compute amoebas). Because there are three components in the amoeba complement, there are three convergent Laurent series expansions of $F(x, y)$. Consider the power series expansion $F(x, y) = \sum_{i,j\geq 0} \binom{i+j}{i} x^i y^j$, corresponding to the component of the amoeba complement that lies in the third quadrant. Since

$$\sum_{i,j\geq 0} \left| \binom{i+j}{i} x^i y^j \right| = \sum_{i,j\geq 0} \binom{i+j}{i} |x|^i |y|^j = \frac{1}{1 - |x| - |y|}, \tag{7.3}$$

https://doi.org/10.1017/9781108874144.012 Published online by Cambridge University Press

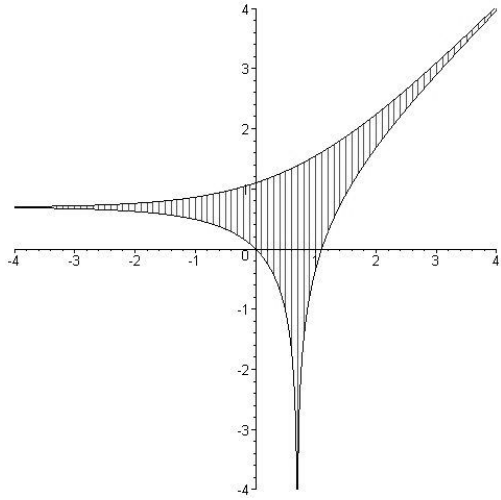

Figure 7.1 Amoeba of the function $1 - x - y$.

this series expansion has domain of convergence $\mathcal{D} = \{(x, y) \in \mathbb{C}^2 : |x| + |y| < 1\}$. For any $a, b \in (0, 1)$ with $a + b < 1$ we can write

$$\begin{aligned} \binom{i+j}{i} &= \frac{1}{(2\pi i)^2} \int_{\mathbf{T}(a,b)} \frac{1}{1-x-y} \frac{dxdy}{x^{i+1}y^{j+1}} \\ &= \frac{1}{(2\pi i)^2} \int_{\mathbf{T}(a,b)} \frac{1}{1-x-y} e^{-\phi(x,y)} \frac{dxdy}{xy}, \end{aligned} \tag{7.4}$$

where $\phi(x, y) = i \log x + j \log y$. We aim to use residue computations to reduce the two-dimensional integral (7.4) to a one-dimensional integral over some path in the singular set $\mathcal{V} = \{(x, y) \in \mathbb{C}^2 : x + y = 1\}$, and then compute a saddle point integral. Thus, we set $y = 1 - x$ in $\phi(x, y)$ and solve for a saddle point, where the first derivative of the function vanishes. The equation

$$0 = \frac{d}{dx}\phi(x, 1-x) = \frac{i}{x} - \frac{j}{1-x}$$

implies $x = i/(i + j)$. Hence, we aim to determine asymptotic behavior by studying the Cauchy integral near $(x_*, y_*) = (i/(i + j), j/(i + j)) \in \mathcal{V}$. For this discussion we fix positive integers $r, s > 0$ and derive asymptotics of the

https://doi.org/10.1017/9781108874144.012 Published online by Cambridge University Press

coefficient sequence $(i, j) = n(r, s)$ as $n \to \infty$. To that end, define

$$I = \frac{1}{(2\pi i)^2} \int_{|x|=x_*} \left(\int_{|y|=y_*-\varepsilon} \frac{1}{1-x-y} \frac{dy}{y^{ns+1}} \right) \frac{dx}{x^{nr+1}}$$

$$I_{\text{loc}} = \frac{1}{(2\pi i)^2} \int_{\mathcal{N}} \left(\int_{|y|=y_*-\varepsilon} \frac{1}{1-x-y} \frac{dy}{y^{ns+1}} \right) \frac{dx}{x^{nr+1}}$$

$$I_{\text{out}} = \frac{1}{(2\pi i)^2} \int_{\mathcal{N}} \left(\int_{|y|=y_*+\varepsilon} \frac{1}{1-x-y} \frac{dy}{y^{ns+1}} \right) \frac{dx}{x^{nr+1}},$$

where $\mathcal{N} = \{x \in \mathbb{C} : |x| = x_* \text{ and } \arg(x) \in (-\delta, \delta)\}$ is any arbitrarily small neighborhood of x_* in the circle $\{|x| = x_*\}$. As we will see in Chapter 9, both $I - I_{\text{loc}}$ and I_{out} grow exponentially slower than I, so (7.4) implies

$$\binom{nr+ns}{rn} = I = I_{\text{loc}} - I_{\text{out}} + \text{exponentially negligible term.}$$

Thus, we can use the (univariate) residue theorem to approximate $\binom{nr+ns}{rn}$ by

$$\begin{aligned} I_{\text{loc}} - I_{\text{out}} &= \frac{1}{(2\pi i)^2} \int_{\mathcal{N}} \left(\int_{|y|=y_*-\varepsilon} \frac{1}{1-x-y} \frac{dy}{y^{ns+1}} - \int_{|y|=y_*+\varepsilon} \frac{1}{1-x-y} \frac{dy}{y^{ns+1}} \right) \frac{dx}{x^{nr+1}} \\ &= \frac{-1}{(2\pi i)} \int_{\mathcal{N}} \operatorname*{Res}_{y=1-x} \frac{y^{-ns-1}}{1-x-y} \frac{dx}{x^{nr+1}} \\ &= \frac{1}{(2\pi i)} \int_{\mathcal{N}} \frac{dx}{x^{nr+1}(1-x)^{ns+1}}. \end{aligned}$$

Making the change of variables $x = x_* e^{i\theta}$ results in the saddle point integral

$$I_{\text{loc}} - I_{\text{out}} = \frac{x_*^{-rn} y_*^{-sn}}{2\pi} \int_{-\delta}^{\delta} A(\theta) e^{-n\phi(\theta)},$$

where

$$A(\theta) = \frac{1}{1 - x_* e^{i\theta}} = \frac{r+s}{s} + O(\theta)$$

and

$$\phi(\theta) = r \log(x_* e^{i\theta}) + s \log(1 - x_* e^{i\theta}) - r \log(x_*) - s \log(y_*) = \frac{r(r+s)}{2s} \theta^2 + O\left(\theta^3\right).$$

Theorem 4.1 from Chapter 4 then gives an asymptotic expansion

$$\binom{nr+ns}{nr} = \left(\frac{r+s}{r}\right)^{rn} \left(\frac{r+s}{s}\right)^{sn} n^{-1/2} \left(\frac{\sqrt{r+s}}{2rs\pi n} + \cdots \right).$$

◁

https://doi.org/10.1017/9781108874144.012 Published online by Cambridge University Press

The approach taken in Example 7.2 is known as the ***surgery method*** for multivariate asymptotics. It works by performing an explicit deformation to move the torus of integration in the Cauchy integral near a critical point, then changing the radius in one coordinate to enclose singularities. The ordinary (univariate) residue theorem, a localization argument, and the saddle point results from Chapters 4 and 5 then yield asymptotics.

Although this approach can be generalized successfully, as will be done in Section 9.1 of Chapter 9, such explicit deformations require additional assumptions on the singularities where local behavior of $F(\boldsymbol{z})$ determines asymptotics. In particular, such singularities need to be *minimal* in the sense of Section 6.4, meaning they lie on the boundary of the domain of convergence of the Laurent expansion being considered. In fact, we require *finite minimality*, meaning such singularities are minimal and only a finite number of other singularities have the same coordinatewise modulus. Although this is usually not an unreasonable assumption, in practice it can be very expensive to verify formally (see Chapter 8 for more details).

Exercise 7.1. Suppose we perturb Example 7.2 by taking $Q_\varepsilon(x,y) = 1 - x - y - \varepsilon y^2$ for some $\varepsilon > -1$. Let $D_\varepsilon = \{(x,y) \in \mathbb{C}^2 : |x|, |y| < \rho_\varepsilon\}$ where $\rho_\varepsilon = \left(\sqrt{1+\varepsilon} - 1\right)/\varepsilon$ the positive root of $Q_\varepsilon(x,x)$. When $\varepsilon = 0$, the function $1/Q_\varepsilon(x,y)$ is the function in (7.3), whose power series domain of convergence contains $D_0 = \{(x,y) \in \mathbb{C}^2 : |x|, |y| < 1/2\}$.

(a) As $\varepsilon \to 0$, determine the first two terms of the asymptotic behavior of ρ_ε.
(b) When $\varepsilon > 0$, is there an easy way to see that $1/Q(x,y)$ is analytic on D_ε?
(c) When $-1 < \varepsilon < 0$, can you show that $1/Q(x,y)$ is analytic on D_ε?
(d) What can you say when $\varepsilon \leq -1$?

We now study an example where the surgery method does not directly apply, and sketch a more general ***topological method*** for multivariate asymptotics. Although the topological method applies in a wider variety of situations, as its name suggests it will require more advanced constructions from topology and differential geometry. Our next example also illustrates how the topological approach generalizes hands-on surgery in the smooth case to a topologically characterized contour integration.

Example 7.3 (Non-Minimal Contributing Points)**.** Consider the $(1,1)$-diagonal sequence $a_{n,n}$ of the power series expansion

$$F(x,y) = \frac{1}{Q(x,y)} = \sum_{i,j \geq 0} a_{i,j} x^i y^j,$$

https://doi.org/10.1017/9781108874144.012 Published online by Cambridge University Press

where $Q(x,y) = (1-x-y)(1+3x)$, so

$$a_{i,j} = \sum_{k=0}^{i} \binom{k+j}{k} (-3)^{i-k}.$$

The singular set $\mathcal{V} = \mathcal{V}_Q$ is the union of the hyperplane $\mathcal{V}_{1-x-y}$ from Example 7.2 with the hyperplane $\mathcal{V}_{1+3x}$. It contains the point $(x_{**}, y_{**}) = (-1/3, 4/3)$ on the intersection of the hyperplanes where $\mathcal{V}$ is not a manifold.

Since $\mathcal{V}$ still contains the hyperplane $\mathcal{V}_{1-x-y}$, the point $(x_*, y_*) = (1/2, 1/2)$ identified in Example 7.2 is still of interest for the asymptotic analysis. Furthermore, the topology of $\mathcal{V}$ changes at the non-smooth point (x_{**}, y_{**}), so this point is also of interest. The function $\phi(x,y) = \log x + \log y$ has nonvanishing derivative when restricted to $\mathcal{V}_{1+3x}$, hence there are no other points where we could restrict the Cauchy integrand to the singular variety and get a saddle point integral.

As we will see later, asymptotics of the coefficient sequence $a_{n,n}$ are still determined by reducing to an integral near (x_*, y_*). However, unlike Example 7.2 we cannot simply move the contour of integration in the Cauchy integral

$$a_{n,n} = \frac{1}{(2\pi i)^2} \int_{|x|=\varepsilon_1} \int_{|y|=\varepsilon_2} \frac{1}{(1-x-y)(1+3x)} \frac{dxdy}{x^{n+1}y^{n+1}}$$

to a torus $\{(x,y) : |x| = x_*, |y| = y_* - \varepsilon\}$ as we would cross the singular set $\mathcal{V}$ at points where $x = -1/3$. To work around this, we expand y *through* the singular variety, resulting in an integral over a tube around $\mathcal{V}_{1-x-y}$, reduce to an integral on $\mathcal{V}_{1-x-y}$ through a residue computation, and *then* move the contour of integration to the saddle point.

For concreteness, we now take $\varepsilon_1 = \varepsilon_2 = 1/10$, although any positive values satisfying $0 < \varepsilon_1 + \varepsilon_2 < 1$ and $\varepsilon_1 < 1/3$ would work. Let $T_0 = \{|x| = |y| = 1/10\}$ and, for any $M > 0$, define the map

$$\begin{aligned} K_M : T_0 \times [0,1] &\to \mathbb{C}^2 \\ (x,y,t) &\mapsto (x,\ y(1+Mt)) \,. \end{aligned}$$

Then K_M is a homotopy from T_0 to the torus $T_1 = \{|x| = 1/10, |y| = (M+1)/10\}$. As long as $M > 10$ then $F(x,y)$ is analytic on T_0 and T_1, the image of K_M does not intersect the coordinate axes of $\mathbb{C}^2$, and this image intersects $\mathcal{V}$ in the set $C = \{(x, 1-x) : |x| = 1/10\}$. Furthermore, the image of K_M intersects $\mathcal{V}$ *transversely*, meaning the tangent planes of these sets jointly span $\mathbb{C}^2$ at their common points. See Figure 7.2 for a visualization of the path of this homotopy after taking the Relog map.

Because $F(x,y)$ is analytic on $\mathbb{C}^2 \setminus \mathcal{V}$, Stokes's Theorem (Theorem A.24 in

https://doi.org/10.1017/9781108874144.012 Published online by Cambridge University Press

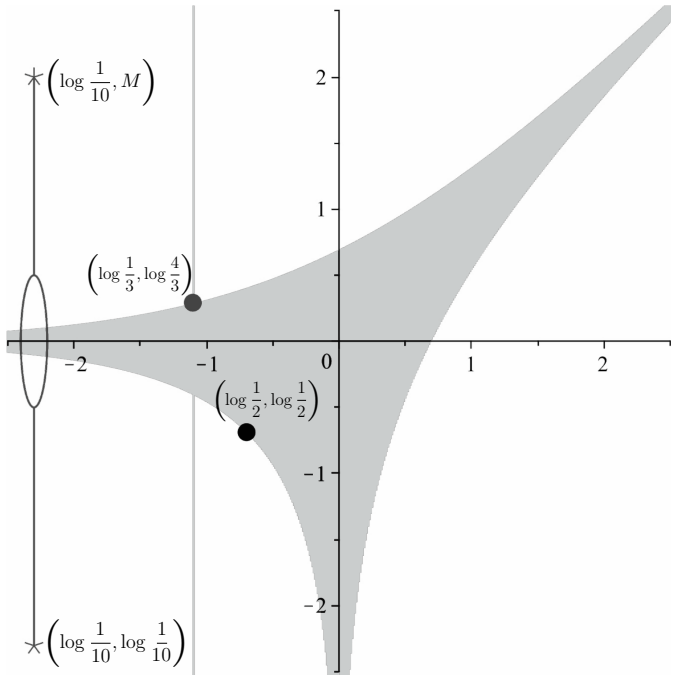

Figure 7.2 The amoeba of $(1 - x - y)(1 + 3x)$. We start by integrating over the torus defined by $|x| = 1/10$ and $|y| = 1/10$ and expand $|y|$ to $(M + 1)/10 > 11/10$, resulting in an integral over a *tubular neighborhood* of $\mathcal{V}$. Taking a residue reduces to an integral over a curve lying on the hyperplane $1 - x - y = 0$ then, avoiding the set of points where $1 + 3x = 0$, we slide this contour to a curve near the point $(1/2, 1/2)$ on $\mathcal{V}$ together with points that do not affect dominant asymptotics.

Appendix A) implies that the Cauchy integral over the boundary of any 3-cycle in $\mathbb{C}^2_* \setminus \mathcal{V}$ is zero. In particular,

$$\int_{T_0} F(x,y)\frac{dxdy}{x^{n+1}y^{n+1}} = \int_{\nu} F(x,y)\frac{dxdy}{x^{n+1}y^{n+1}} + \int_{T_1} F(x,y)\frac{dxdy}{x^{n+1}y^{n+1}}\,, \qquad (7.5)$$

where ν is a ***tubular neighborhood*** of C: the union of circles normal to the tangent plane of $\mathcal{V}$ with centers at the points of C (see Figure 7.3). Furthermore, because (7.5) holds for any $M > 10$, and

$$\int_{T_1} F(x,y)\frac{dxdy}{x^{n+1}y^{n+1}} = O\left(10^n(M+1)^{-n}\right),$$

https://doi.org/10.1017/9781108874144.012 Published online by Cambridge University Press

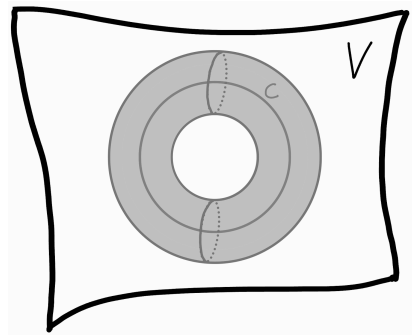

Figure 7.3 A visualization of the tubular neighborhood ν.

taking $M \to \infty$ shows that the integral over T_1 is zero for $n > 0$, and thus

$$a_{n,n} = \frac{1}{(2\pi i)^2} \int_{\nu} F(x,y) \frac{dxdy}{x^{n+1}y^{n+1}} = \frac{1}{(2\pi i)^2} \int_{\nu} \frac{1}{(1-x-y)(1+3x)} \frac{dxdy}{x^{n+1}y^{n+1}}.$$

The tubular neighborhood ν is the union of circles with centers on C, and each point of C corresponds to a simple pole of $F(x,y)$, where $1-x-y=0$, so a generalization of the classical univariate residue theorem implies

$$\begin{aligned} a_{n,n} &= \frac{1}{2\pi i} \int_{|x|=1/10} \operatorname*{Res}_{y=1-x} \frac{1}{(1-x-y)(1+3x)} \frac{dx}{x^{n+1}y^{n+1}} \\ &= \frac{1}{2\pi i} \int_{|x|=1/10} \frac{1}{1+3x} \frac{dx}{x^{n+1}(1-x)^{n+1}}. \end{aligned} \tag{7.6}$$

As in the last example, the integrand of (7.6) becomes a saddle point integral near $x = 1/2$. The difference is that while we previously used a residue to localize near the saddle point, this time we took a more "convenient" residue and obtained a univariate integral away from the saddle point. Because we are dealing with an integrand having a linear denominator, we can move our domain of integration to pass through the critical point without much difficulty. We now describe three methods for doing this, listed in decreasing order of explicitness but increasing order of generality.

Method One: Because the only singularity of the integrand in (7.6) between the circles $|x| = 1/10$ and $|x| = 1/2$ occurs at $x = -1/3$, the domain of integration in (7.6) can be replaced by the union of the circle $|x| = 1/2$ and a sufficiently small clockwise circle around $x = -1/3$ (see Figure 7.4 left). The

https://doi.org/10.1017/9781108874144.012 Published online by Cambridge University Press

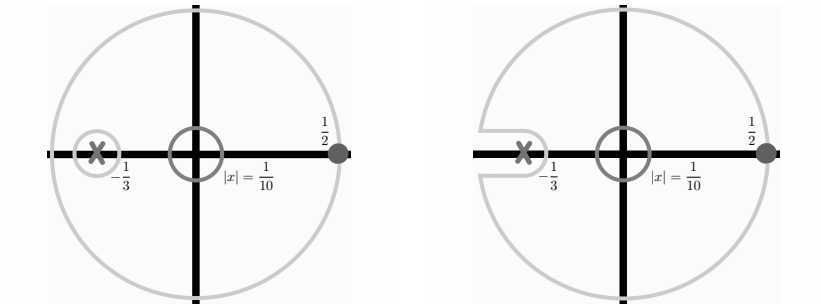

Figure 7.4 *Left:* The circle $|x| = 1/10$ can be expanded to $|x| = 1/2$ by introducing a circle around $x = -1/3$. This results in an extra residue integral which is exponentially negligible. *Right:* Alternatively, we can expand from $|x| = 1/10$ to hit $x = 1/2$ while stopping the increase in an arbitrarily small circle around $x = -1/3$.

residue theorem then implies

$$\begin{aligned} a_{n,n} &= \frac{1}{2\pi i}\int_{|x|=1/2} \frac{1}{1+3x}\frac{dx}{x^{n+1}(1-x)^{n+1}} + \frac{1}{2\pi i}\int_{|x+1/3|=\varepsilon} \frac{1}{1+3x}\frac{dx}{x^{n+1}(1-x)^{n+1}} \\ &= \frac{1}{2\pi i}\int_{|x|=1/2} \frac{1}{1+3x}\frac{dx}{x^{n+1}(1-x)^{n+1}} - \operatorname*{Res}_{x=-1/3}(x+1/3)^{-1}\frac{1/3}{x^{n+1}(1-x)^{n+1}} \\ &= \frac{1}{2\pi i}\int_{|x|=1/2} \frac{1}{1+3x}\frac{dx}{x^{n+1}(1-x)^{n+1}} - \frac{1}{3}\left(\frac{9}{4}\right)^{n+1}, \end{aligned}$$

and a change of variables yields the saddle point approximation

$$\begin{aligned} a_{n,n} &= \frac{4^n}{2\pi}\int_{-\pi}^{\pi} \frac{1}{(1+3e^{i\theta}/2)(1-e^{i\theta}/2)} e^{-ni\theta - n\log(2-e^{i\theta})} d\theta - \frac{1}{3}\left(\frac{9}{4}\right)^{n+1} \\ &= \frac{4^n}{\sqrt{\pi n}}\left(\frac{2}{5} + O\left(\frac{1}{n}\right)\right). \end{aligned}$$

Method Two: In general we cannot work around other singularities by taking residues in such an explicit manner. Although this means we cannot get an explicit representation for error terms coming from other singularities, all we really need to determine dominant asymptotics is to bound any potential asymptotic contributions from these singularities. The only factor of the integrand in (7.6) that depends on n is $x^{-n}(1-x)^{-n}$, so when n is large the modulus of the integrand is well approximated by $e^{nh(x)}$, where

$$h(x) = -\log|x| - \log|1-x|.$$

https://doi.org/10.1017/9781108874144.012 Published online by Cambridge University Press

Points with smaller *height h* make the integrand of (7.6) exponentially smaller, so up to an exponentially negligible error we can ignore points with height bounded below $h(1/2) = \log 4$. Since $h(-1/3) = \log(9/4)$ we could proceed by expanding the circle $|x| = 1/10$ to the circle $|x| = 1/2$ while stopping in a tubular shape around $x = -1/3$ (see Figure 7.4 right). The integral over the resulting curve can be truncated to a neighborhood of $x = 1/2$ in $|x| = 1/2$ while introducing an exponentially negligible error. The integral over this neighborhood of $x = 1/2$ is again a saddle point integral.

Method Three: Although Method Two is more general than Method One, it still requires that we know how to explicitly deform around $\mathcal{V}$, which is not always possible. We thus move to an even more general argument, which will be fully described below. The key is to use the local geometry of $\mathcal{V}$ to describe how to move the domain of integration $|x| = 1/10$ to heights below $h(1/2) = \log 4$, except in a neighborhood of $x = 1/2$, while avoiding $\mathcal{V}$. This is accomplished using a *gradient flow*. Writing $x = a + ib$ for real variables a and b, so that $|x| = \sqrt{a^2 + b^2}$, we see that

$$h(a, b) = h(a + ib) = -\log\left(a^2 + b^2\right)/2 - \log\left((1 - a)^2 + b^2\right)/2.$$

We want to move an arbitrary point $a_\theta + ib_\theta = e^{i\theta}/10$ on our starting circle $|x| = 1/10$ down to points on $\mathcal{V}$ of lower height with respect to h. Since $(\nabla h)(a, b)$ gives the direction of greatest increase of h, we want to locally move a point (a_θ, b_θ) along the direction $-(\nabla h)(a_\theta, b_\theta)$. In other words, we want to solve the first-order differential system of equations

$$\begin{pmatrix} a'_\theta(t) \\ b'_\theta(t) \end{pmatrix} = -\nabla h(a_\theta(t), b_\theta(t)), \qquad a_\theta(0) = \cos(\theta)/10, \qquad b_\theta(0) = \sin(\theta)/10$$

for $a_\theta(t)$ and $b_\theta(t)$. Figure 7.5 shows the trajectories of points under this (negative) gradient flow. Here it can be verified in a computer algebra system that under the flow all points will go below height $h(1/2) = \log 4$, except in a neighborhood of $x = 1/2$. Near $x = 1/2$ the flow approaches a vertical line, ultimately resulting in a saddle point integral. The key reason this method can be generalized is that techniques from Morse theory allow us to know when such a flow exists, and characterize the resulting domains of integration, *without having to actually compute them*.

◁

In our last example the non-smooth point did not affect dominant asymptotics, but this will not always be the case.

Example 7.4 (Dealing with Multiple Points)**.** Consider now asymptotics in the

https://doi.org/10.1017/9781108874144.012 Published online by Cambridge University Press

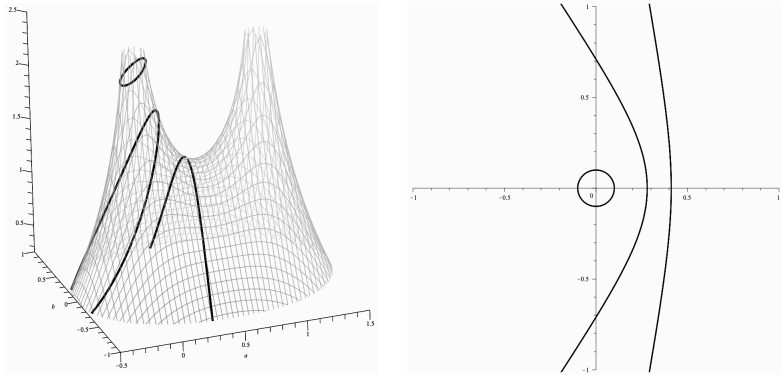

Figure 7.5 *Left:* The gradient flow of $|x| = 1/10$ at three points in time, plotted on $\mathbb{C}^2 \setminus \{0, 1\}$ when arranged by height $h(x) = h(a + ib)$. *Right:* The curves under the flow plotted in the complex plane.

main diagonal direction $\boldsymbol{r} = (1, 1)$ of the power series expansion of $F(x, y) = 1/Q(x, y)$ with $Q(x, y) = (1 - x - y)(1 - 3x)$. The factor $1 - x - y$ is the same as in the above examples, but having the second factor change from $1 + 3x$ to $1 - 3x$ moves the non-smooth point to $(1/3, 2/3)$. Because the height $h(x, y) = -\log x - \log y$ is now larger at $(1/3, 2/3)$ than $(1/2, 1/2)$, we can no longer easily rule out the non-smooth point. In fact, following Method One from the last example shows

$$\begin{aligned} a_{n,n} &= \frac{1}{2\pi i} \int_{|x-1/3|=\varepsilon} \frac{1}{1-3x} \frac{dx}{x^{n+1}(1-x)^{n+1}} + \frac{1}{2\pi i} \int_{|x|=1/2} \frac{1}{1-3x} \frac{dx}{x^{n+1}(1-x)^{n+1}} \\ &= \operatorname*{Res}_{x=1/3} (x - 1/3)^{-1} \frac{1/3}{x^{n+1}(1-x)^{n+1}} + \frac{1}{2\pi i} \int_{|x|=1/2} \frac{1}{1+3x} \frac{dx}{x^{n+1}(1-x)^{n+1}} \\ &= \frac{1}{3} \left(\frac{9}{2} \right)^{n+1} + O(4^n). \end{aligned}$$

More generally, if $\mathcal{V}$ is no longer a manifold then we compute a *Whitney stratification*, partitioning $\mathcal{V}$ into a finite collection of manifolds such that the local geometry of $\mathcal{V}$ is consistent near the points in any fixed element of the partition. We then perform an analysis similar to the smooth case on each of the manifolds, obtaining a set of equations for each manifold that characterizes the points of interest for our asymptotic calculations. The asymptotic contribution of such a point depends on the geometry near the singularity. In this text we study singularities where $\mathcal{V}$ is locally smooth (in Chapter 9), looks like the union of hyperplanes (in Chapter 10), or looks like a cone point (in

https://doi.org/10.1017/9781108874144.012 Published online by Cambridge University Press

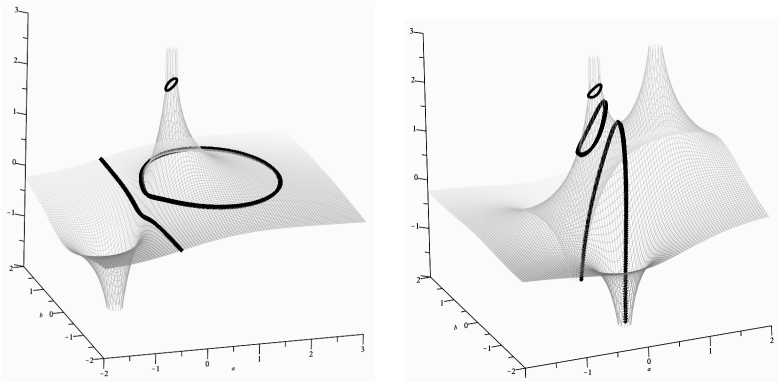

Figure 7.6 The gradient flow of $|x| = 1/10$ at three points in time, plotted on $\mathbb{C}^2 \setminus \{0, 1\}$ when arranged by height $h(x) = h(a + ib)$. *Left:* The flow on $\mathcal{V}_{1-y-xy}$. *Right:* The flow on $\mathcal{V}_{1-x-y-x^2y}$.

Chapter 11). Studying flows on general algebraic varieties requires us to adapt tools from *stratified* Morse theory. ◁

Exercise 7.2. Sketch the vector field $-(\nabla h)(a, b)$ on the right-hand side of Figure 7.5.

Gradient flows form an important component of our analytic toolbox. Indeed, rather than computing a flow for each example, standard results in Morse theory usually guarantee the existence of flows that push domains of integration down to points where saddle point approximations can be computed. Unfortunately, these results require the height map to be *proper* (meaning that the set of points with height in a closed interval is compact). Because this properness condition is usually not satisfied in our setting, it is possible for the desired flows not to exist.

Example 7.5 (Critical Points at Infinity)**.** Consider the diagonal sequences $a_{n,n}$ of the power series expansions of $1/A(x, y)$ and $1/B(x, y)$, where $A(x, y) = 1 - y - xy$ and $B(x, y) = 1 - x - y - x^2y$. The negative gradient flows of the circle $|x| = 1/10$ on $\mathcal{V}_A$ and $\mathcal{V}_B$ are shown in Figure 7.6. Because $y = 1/(x + 1)$ on $\mathcal{V}_A$, the product $xy = x/(x + 1) \to 1$ as $x \to \infty$, and thus the height function $h(x, y) = -\log|x| - \log|y| \to 0$ as $x \to \infty$ on $\mathcal{V}_A$. Since $h(x, y)$ can stay bounded as (x, y) goes to infinity, the height function is not proper. As seen in the left of Figure 7.6, the circle $|x| = 1/10$ stays at bounded height but never reaches a saddle. In fact, $\mathcal{V}_A$ contains no saddles, and we say that it has a *critical point at infinity*.

https://doi.org/10.1017/9781108874144.012 Published online by Cambridge University Press

Similarly, because $y = (1-x)/(1+x^2)$ on $\mathcal{V}_B$, the height function $h(x,y)$ approaches zero as $x \to \infty$ on $\mathcal{V}_B$. However, on $\mathcal{V}_B$ the circle $|x| = 1/10$ does flow to a saddle point of height greater than zero. Again we have a critical point at infinity, but this time it is of lower height than an actual saddle point on the variety. Thus, non-properness of the height function does not preclude an asymptotic analysis, as we can ignore points of height bounded below the saddle point if we care only about dominant asymptotic behavior. ◁

In Section 7.5 we discuss computable conditions, often satisfied in practice, that imply the conclusions of Morse theory we require apply even without a proper height function.

Exercise 7.3. Let $Q(x,y) = 1-x-y-x^2y^2$ and $h_{\boldsymbol{r}}(x,y) = -r_1 \log|x| - r_2 \log|y|$ be the height function corresponding to the $\boldsymbol{r}$-diagonal sequence $(a_{r_1 n, r_2 n})$. Prove that when $\boldsymbol{r} = (2,1)$ the height function $h_{\boldsymbol{r}}(x,y)$ approaches a finite limit as $y \to \infty$ and $x \to 0$, and evaluate the limit. Prove that when $\boldsymbol{r} = (1,1)$ the height function $h_{\boldsymbol{r}}(x,y)$ has no finite limit as either x or y goes to infinity.

7.2 The smooth case

We now generalize the above argument to any rational function whose singular variety $\mathcal{V}$ is a complex manifold. The ***square-free part*** $\tilde{Q}$ of the polynomial Q is the product of its distinct irreducible factors over the complex numbers, and we say that Q is ***square-free*** if $\tilde{Q} = Q$. We call $\boldsymbol{z} \in \mathcal{V}$ a ***smooth point*** if $\nabla \tilde{Q}(\boldsymbol{z})$ is non-zero, and say that $\mathcal{V}$ is ***smooth*** if $\tilde{Q}$ and all its partial derivatives never simultaneously vanish. The implicit function theorem implies that a smooth singular variety can be viewed both as a $(d-1)$-dimensional complex manifold and as a $(2d-2)$-dimensional real manifold, and both of these viewpoints will be beneficial. We introduce the square-free part of Q so that the converse also holds.

Lemma 7.6. *The inequality $\nabla \tilde{Q}(\boldsymbol{z}) \neq \mathbf{0}$ holds for a point $\boldsymbol{z} \in \mathcal{V}_Q$ if and only if $\mathcal{V}$ is a smooth manifold in a neighborhood of $\boldsymbol{z}$.*

Proof Sketch The forward implication follows from the implicit function theorem. The converse, that $\nabla \tilde{Q}(\boldsymbol{z}) = \mathbf{0}$ implies a geometric singularity, is harder to prove. Let $m_{\boldsymbol{x}}$ denote the maximal ideal of functions vanishing at $\boldsymbol{x}$ in the ring of polynomial functions vanishing on $\mathcal{V}$, and let $n_{\boldsymbol{x}}$ denote the maximal ideal of functions vanishing at $\boldsymbol{x}$ in the ring of germs of analytic functions at $\boldsymbol{x}$ (as defined in Definition 10.42 below). Then $\nabla \tilde{Q}(\boldsymbol{x}) = \mathbf{0}$ implies $m_{\boldsymbol{x}}/m_{\boldsymbol{x}}^2$ has dimension d rather than $d-1$ (see [Sha13, Exercise 2.2 and Theorem 2.1])

https://doi.org/10.1017/9781108874144.012 Published online by Cambridge University Press

so that $n_{\boldsymbol{x}}/n_{\boldsymbol{x}}^2$ has dimension d, and this property is invariant under bi-analytic mapping. At any smooth point of a complex hypersurface there is a coordinate neighborhood taking $\boldsymbol{x}$ to the origin and making the hypersurface into the coordinate plane where $z_1 = 0$. In this case $n_{\mathbf{0}}/n_{\mathbf{0}}^2$ has dimension $d-1$, which would be a contradiction, hence $\mathcal{V}$ is not a complex manifold in a neighborhood of $\boldsymbol{x}$. A little more work shows $\mathcal{V}$ is not locally a C^∞-manifold either. □

Our starting point, as always, is the multivariate Cauchy Integral Formula

$$a_{\boldsymbol{r}} = \left(\frac{1}{2\pi i}\right)^d \int_T \boldsymbol{z}^{-\boldsymbol{r}-\mathbf{1}} F(\boldsymbol{z})\, d\boldsymbol{z}\,, \tag{7.7}$$

which gives an exact representation for $a_{\boldsymbol{r}}$. We view this representation not as a standard integral from multivariate calculus, but as the integral of the differential form $\omega = \boldsymbol{z}^{-\boldsymbol{r}-\mathbf{1}} F(\boldsymbol{z})\, d\boldsymbol{z}$ over the d-chain T. The necessary background on differential geometry and the basics of integration of forms is discussed in Appendix A. Appendix B reviews concepts from algebraic topology, including homology and cohomology classes. In particular, since $\mathcal{M} = \mathbb{C}_*^d \setminus \mathcal{V}$ is the domain of holomorphicity for ω, the Cauchy integral depends only on the class of T in the singular homology group $H_d(\mathcal{M})$ and the class of ω in the singular cohomology group $H^d(\mathcal{M})$.

We break our argument into pieces, generally mirroring the final approach to Example 7.3 above. In this chapter we mainly stick to theoretical considerations; methods for computing the quantities that arise are discussed in Chapter 8.

Step 1: Characterize critical points

We begin by defining the ***height function***

$$h_{\boldsymbol{r}}(\boldsymbol{z}) := -\boldsymbol{r} \cdot \operatorname{Relog} \boldsymbol{z} = -\sum_{j=1}^{d} r_j \log|z_j|\,,$$

which captures the magnitude of the Cauchy integrand

$$\left|\boldsymbol{z}^{-\boldsymbol{r}-\mathbf{1}} F(\boldsymbol{z})\right| = e^{|\boldsymbol{r}|\, h_{\hat{\boldsymbol{r}}}(\boldsymbol{z})} \cdot \left|\boldsymbol{z}^{-\mathbf{1}} F(\boldsymbol{z})\right|$$

as $\left|\boldsymbol{z}^{-\mathbf{1}} F(\boldsymbol{z})\right|$ independent of $|\boldsymbol{r}|$. The ordering $h_{\boldsymbol{r}}$ gives to $\mathbb{C}_*^d$ does not change if $\boldsymbol{r}$ is multiplied by a positive scalar, so our arguments about the height function will hold whenever $\boldsymbol{r}$ is replaced by any positive multiple. This invariance property means that an analysis of $a_{\boldsymbol{r}}$ as $\boldsymbol{r} \to \infty$ with $\hat{\boldsymbol{r}} = \boldsymbol{r}/|\boldsymbol{r}|$ converging to some fixed $\hat{\boldsymbol{r}}_*$ can usually be accomplished with the fixed height function $h_{\hat{\boldsymbol{r}}_*}$. In particular, if $\hat{\boldsymbol{r}}_*$ is a fixed direction and $h_{\boldsymbol{r}_*}(\boldsymbol{x}) < h_{\boldsymbol{r}_*}(\boldsymbol{y})$ then, as $\boldsymbol{r} \to \infty$ with $\hat{\boldsymbol{r}} \to \boldsymbol{r}_*$, the Cauchy integrand is exponentially smaller at $\boldsymbol{z} = \boldsymbol{x}$ than at $\boldsymbol{z} = \boldsymbol{y}$. When $\boldsymbol{r}$ is understood we write simply h for $h_{\boldsymbol{r}}$.

https://doi.org/10.1017/9781108874144.012 Published online by Cambridge University Press

Definition 7.7. A ***smooth critical point*** $\boldsymbol{z}$ of the rational function $F = P/Q$ in the direction $\hat{\boldsymbol{r}}$ is a smooth point of $\mathcal{V}_*$ that is a critical point of $h_{\hat{\boldsymbol{r}}} : \mathcal{V}_* \to \mathbb{R}$ as a smooth mapping of real manifolds. The set of critical points in the direction $\hat{\boldsymbol{r}}$ is denoted by $\texttt{critical}(\boldsymbol{r})$.

The height function $h_{\hat{\boldsymbol{r}}}$ is the real part of (a branch of) the analytic function $\phi(\boldsymbol{z}) = -\boldsymbol{r} \cdot \log \boldsymbol{z}$, and the Cauchy–Riemann equations imply that the critical points of F in the direction $\hat{\boldsymbol{r}}$ can also be computed as the critical points of $\phi : \mathcal{V}_* \to \mathbb{C}$ as a (locally) holomorphic mapping of complex manifolds. In particular, we have the following explicit definition of smooth critical points.

Lemma 7.8. *Assume that $\mathcal{V}$ is a smooth manifold and let $\tilde{Q}$ be the square-free part of the denominator Q. Then $\boldsymbol{w} \in \mathbb{C}_*^d$ is a critical point in the direction $\hat{\boldsymbol{r}}$ if and only if it satisfies the* ***smooth critical point equations***

$$\tilde{Q}(\boldsymbol{w}) = r_k w_1 \tilde{Q}_{z_1}(\boldsymbol{w}) - r_1 w_k \tilde{Q}_{z_k}(\boldsymbol{w}) = 0 \qquad (2 \le k \le d)\,, \tag{7.8}$$

where $\tilde{Q}_{z_j}$ denotes the derivative of $\tilde{Q}$ with respect to the variable z_j.

Proof The point $\boldsymbol{w}$ is a critical point when $Q(\boldsymbol{w}) = 0$ and the differential of $\phi : \mathcal{V}_* \to \mathbb{C}$ is zero. Vanishing of this differential occurs exactly when the differential of ϕ as a map from $\mathbb{C}_*^d$ to $\mathbb{C}$ projects to zero on the tangent space of $\mathcal{V}_*$ at $\boldsymbol{w}$. Since the tangent space to $\mathcal{V}_*$ at $\boldsymbol{w}$ is the hyperplane with normal $(\nabla \tilde{Q})(\boldsymbol{w})$, the differential of ϕ projects to zero if and only if $(\nabla \phi)(\boldsymbol{w})$ is parallel to $(\nabla \tilde{Q})(\boldsymbol{w})$. These vectors are parallel if and only if all 2×2 minors of the matrix

$$\begin{pmatrix} \left(\nabla \tilde{Q}\right)(\boldsymbol{w}) \\ (\nabla \phi)(\boldsymbol{w}) \end{pmatrix} = \begin{pmatrix} \tilde{Q}_{z_1}(\boldsymbol{w}) & \cdots & \tilde{Q}_{z_d}(\boldsymbol{w}) \\ -r_1/w_1 & \cdots & -r_d/w_d \end{pmatrix}$$

vanish. Vanishing of the minors simplifies to give the smooth critical point equations. □

Remark 7.9. The smooth critical point equations (7.8) form a polynomial system with d equations in d variables. It is therefore unsurprising that *generically* Q has a finite number of critical points (i.e., this holds for all polynomials Q except for those whose coefficients come from a fixed algebraic set depending only on the degree of Q). This follows directly from an algebraic version of Sard's Theorem, which can be found in [BPR03, Theorem 5.56]; see also [Mel21, Section 5.3.4] for an explicit derivation.

Exercise 7.4. Continuing Exercise 7.3, let $\boldsymbol{r} = (2, 1)$ and find the critical points for $h_{\boldsymbol{r}}$ on $\mathcal{V}$. Compute the heights of these critical points and compare them to the limit height for the sequence approaching infinity in Exercise 7.3. Is the limit height larger than the heights of all critical points on $\mathcal{V}$?

https://doi.org/10.1017/9781108874144.012 Published online by Cambridge University Press

Proposition 7.10. *Singularity of the Hessian matrix for $h_{\hat{r}}$ in local coordinates at a critical point for $h_{\hat{r}}$ on the smooth variety $\mathcal{V}_*$ is independent of the choice of coordinatization of $\mathcal{V}_*$ as a complex manifold.*

Proof At a point $\boldsymbol{p}$ where $\nabla h_{\hat{r}}$ vanishes, the chain rule under a coordinate change Ψ simplifies to $\mathcal{H}' = J_\Psi \mathcal{H}$, where $\mathcal{H}'$ is the new Hessian, $\mathcal{H}$ is the old Hessian, and J_Ψ is the Jacobian matrix of Ψ at $\boldsymbol{p}$. The claim follows from nonsingularity of J_Ψ at $\boldsymbol{p}$. □

Definition 7.11. A smooth critical point $\boldsymbol{w}$ of h is called a ***nondegenerate critical point*** if the Hessian matrix for h in local coordinates around $\boldsymbol{w}$ is nonsingular.

This definition is generalized to non-smooth points in Definition 7.34 below. Under our assumption that $\mathcal{V}$ is smooth, one of the partial derivatives of the square-free part of Q is nonvanishing at $\boldsymbol{w}$. Without loss of generality, we assume that $\tilde{Q}_{z_d}(\boldsymbol{w}) \neq 0$ is non-zero, so we can parametrize $\mathcal{V}$ near $\boldsymbol{w}$ as $z_d = g(\boldsymbol{z}^\circ) = g(z_1, \ldots, z_{d-1})$ for some analytic function g defined in a neighborhood of $\boldsymbol{w}^\circ$. The critical point $\boldsymbol{w}$ is nondegenerate if and only if the Hessian matrix of $h(\boldsymbol{z}^\circ, g(\boldsymbol{z}^\circ))$ with respect to $z_1, \ldots, z_{d-1}$ has non-zero determinant at $\boldsymbol{z}^\circ = \boldsymbol{w}^\circ$. We say h is a ***Morse height function*** when all of its critical points are nondegenerate.

Remark. Most topological works, such as [Mil63; GM88], study spaces using Morse height functions. However, as discussed in Appendix C, as long as there are finitely many critical points the basic Morse decompositions hold whether or not h is Morse: the topology of the space is still generated by attachments at the critical points. However, the description of the attachments becomes more complicated for non-Morse height functions.

Step 2: Intersect the torus with the singular variety

The Cauchy integral representation (7.7) holds for any torus $T = \text{Relog}^{-1}(\boldsymbol{x})$ with $\boldsymbol{x}$ in the component B of $\texttt{amoeba}(Q)^c$ corresponding to the convergent Laurent expansion with coefficients $a_{\boldsymbol{r}}$. We want to replace the domain of integration T with a domain of integration close to $\mathcal{V}$ that "wraps around" the singular variety, so we can use a residue computation in Step 3 below to reduce to an integral "on" $\mathcal{V}$.

If γ is any $(d-1)$-chain in $\mathcal{V}_*$ then the *Collar Lemma* (Lemma C.1 in Appendix C) shows how to construct the *tube* $\texttt{o}\gamma$ *around* γ, which is a d-chain in the domain $\mathcal{M}$ where the Cauchy integral ω is holomorphic. The tube $\texttt{o}\gamma$ can be viewed as a union of circles with centers at the points of γ, and the

https://doi.org/10.1017/9781108874144.012 Published online by Cambridge University Press

map $\gamma \mapsto \mathsf{o}\gamma$ is well defined as a map from the homology group $H_{d-1}(\mathcal{V}_*)$ to $H_d(\mathcal{M})$.

Theorem C.2 of Appendix C implies that $\mathsf{o} : H_{d-1}(\mathcal{V}_*) \to H_d(\mathcal{M})$ is injective, and if T' is any torus contained in $\mathcal{M}$ then pulling back $[T - T'] \in H_d(\mathcal{M})$ via o gives a well-defined class $\mathbf{INT}(T, T') \in H_{d-1}(\mathcal{V}_*)$ known as the *intersection class* of T and T'. By construction, $[T] - [T'] = \mathsf{o}\,\mathbf{INT}(T, T')$ in $H_d(\mathcal{M})$, so that

$$a_{\boldsymbol{r}} = \left(\frac{1}{2\pi i}\right)^d \int_T \omega = \left(\frac{1}{2\pi i}\right)^d \int_{\mathsf{o}\,\mathbf{INT}(T,T')} \omega + \left(\frac{1}{2\pi i}\right)^d \int_{T'} \omega\,.$$

One can picture $\mathsf{o}\,\mathbf{INT}(T, T')$ by imagining a continuous deformation of T to T'. If this deformation is sufficiently generic it will intersect $\mathcal{V}_*$ transversely, with the intersection yielding $\mathbf{INT}(T, T')$. The tube around $\mathbf{INT}(T, T')$ is thus the chain that needs to be added to account for passing the deformation through $\mathcal{V}_*$. See Figure 7.7 for an illustration.

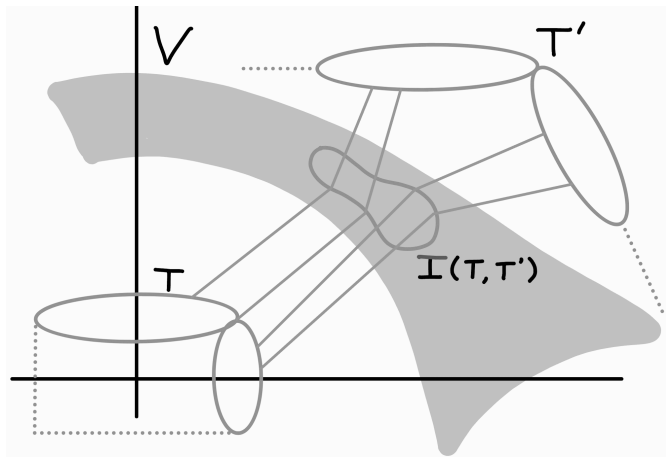

Figure 7.7 An intersection class of T and T' with respect to $\mathcal{V}$.

If we pick a torus T' so that $\int_{T'} \omega = 0$ then we have succeeded in expressing the Cauchy integral as an integral over a tube around a curve in $\mathcal{V}_*$. Corollary 6.29 implies the existence of such a torus, giving the following.

Proposition 7.12. *Assume F is the ratio of coprime polynomials $F(\boldsymbol{z}) = P(\boldsymbol{z})/Q(\boldsymbol{z})$. As $\boldsymbol{r} \to \infty$ in the direction $\hat{\boldsymbol{r}}$ there exists a torus T' such that*

https://doi.org/10.1017/9781108874144.012 Published online by Cambridge University Press

$\int_{T'} \omega = 0$ *for all but finitely many* $\boldsymbol{r}$*, and*

$$a_{\boldsymbol{r}} = \left(\frac{1}{2\pi i}\right)^d \int_{\circ \mathbf{INT}(T,T')} \omega \tag{7.9}$$

whenever the integral over T' *is zero.* □

Exercise 7.5. Let $Q(x, y) = 1 - x - y - x^2y^2$, whose amoeba is shown in Figure 7.8. When $\boldsymbol{r} = (1, 1)$, which components of $\mathtt{amoeba}(Q)^c$ have $h_{\boldsymbol{r}}$ unbounded from below, and which vertices of the Newton polygon for Q do these regions correspond to under the relationship described in Theorem 6.18?

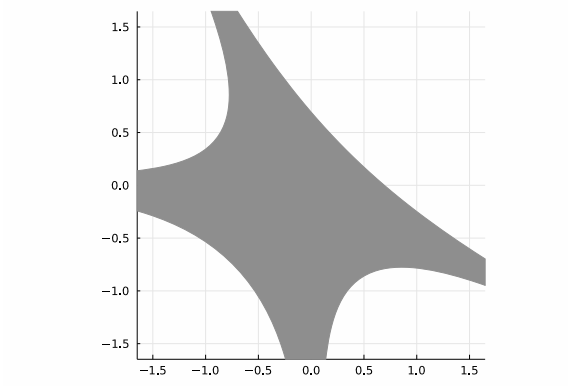

Figure 7.8 Amoeba of $Q(x, y) = 1 - x - y - x^2y^2$.

We can convert the d-dimensional integral in (7.12) to a $(d-1)$-dimensional integral over the intersection cycle, which lies in $\mathcal{V}_*$. This is accomplished using the concept of *multivariate residues* (also called *Leray residues*). Appendix C.2 gives a summary of multivariate residues, but for this discussion it is sufficient to note that the residue form $\mathrm{Res}(\tau)$ of a meromorphic d-form τ with singularities contained in $\mathcal{V}$ is a $(d-1)$ form restricted to $\mathcal{V}$. Theorem C.9 implies that

$$\frac{1}{2\pi i} \int_{\circ\gamma} \tau = \int_{\gamma} \mathrm{Res}(\tau)$$

for any $(d-1)$-chain γ in $\mathcal{V}_*$ and holomorphic d-form τ on $\mathcal{M}$.

In particular, combining the residue operator with Proposition 7.12 gives the following.

https://doi.org/10.1017/9781108874144.012 Published online by Cambridge University Press

Proposition 7.13. *If T' is a torus described by Proposition 7.12 then*

$$a_{\boldsymbol{r}} = \left(\frac{1}{2\pi i}\right)^{d-1} \int_{\mathbf{INT}(T,T')} \operatorname{Res} \omega. \tag{7.10}$$

□

Exercise 7.6. Suppose $d = 1$ and $\mathcal{V} = \mathcal{V}_Q$ where $Q(z) = 2 - 3z + z^2$. Let T be a circle of some small positive radius ε and T' be a circle of some large radius M.

(a) What is the cycle $\mathbf{INT}(T, T')$?
(b) What is the form $\operatorname{Res}(\omega)$ when $\omega = Q(z)^{-1} z^{-n-1} dz$?
(c) What is $\int_{\mathbf{INT}(T,T')} \operatorname{Res}(\omega)$?
(d) What is $\mathsf{o}\,\mathbf{INT}(T, T')$?
(e) Describe in words why $\mathsf{o}\,\mathbf{INT}(T, T')$ is homologous to $T - T'$ in $H_1(\mathbb{C}_* \backslash \mathcal{V})$.

Step 3: Determine a Morse-Theoretic Decomposition of the Singular Variety

Having reduced the Cauchy integral to an integral over an intersection cycle $\gamma = \mathbf{INT}(T, T')$ lying *in* the singular variety $\mathcal{V}_*$, we now want to deform γ in $\mathcal{V}_*$ to represent the coefficient sequence of interest as a sum of saddle point integrals. Because we are currently assuming $\mathcal{V}$ is smooth, we could try to compute such a representation by taking a gradient flow of γ on $\mathcal{V}$ with respect to the height function $h_{\hat{\boldsymbol{r}}}$. If γ can be deformed so that it lies in the neighborhood of a nondegenerate critical point σ of $h_{\hat{\boldsymbol{r}}}$, except for points of height at most $\sigma - \varepsilon$ for some $\varepsilon > 0$, then we can apply the saddle point techniques of Chapter 5 to compute asymptotics (up to an exponentially negligible error, coming from ignoring points of lower height).

Actually computing such a gradient flow on real examples is usually not feasible. Fortunately, one of the most important consequences of Morse theory is that under reasonable conditions *there are only a finite number of possibilities for the long-term behavior of such a flow*. In particular, as detailed in Appendix C and summarized here, if the flow does not stay at bounded height while escaping to infinity on $\mathcal{V}_*$ then we can flow γ until it gets locally "stuck" on one of the critical points of $h_{\hat{\boldsymbol{r}}}$.

Our results are phrased in the language of *singular homology*, reviewed in Appendix B. Of particular use to us are the notions of *relative homology*, which allows us to discuss homology near a critical point while ignoring points

https://doi.org/10.1017/9781108874144.012 Published online by Cambridge University Press

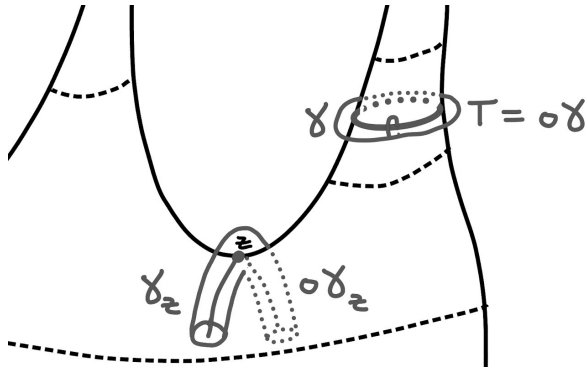

Figure 7.9 The curve γ is deformed to a curve $\gamma_{\boldsymbol{z}}$ locally draped over a saddle $\boldsymbol{z}$ centered at a critical point for the height function. The tubes around γ and $\gamma_{\boldsymbol{z}}$ are also pictured.

of lower height that do not affect dominant asymptotic behavior, and *attachments*, which describe how to decompose the singular variety by joining together topologically simpler spaces. Our discussion here summarizes the main points of the machinery developed in the appendices before applying them to our situation.

Morse theory represents the topology of a manifold X equipped with a smooth map $h : X \to \mathbb{R}$ in terms of successive attachments. The smooth function h is referred to as a *height function* on X. As discussed above, we say h is a *Morse* if its critical points are nondegenerate, and *proper* if the inverse image of any closed interval is compact. Let $X_{\leq c}$ denote the subspace of all points $\boldsymbol{z} \in X$ with $h(\boldsymbol{z}) \leq c$ and suppose that h is a proper Morse function. As described in Section C.3 of Appendix C, Morse theory describes the change in topology when the space $X_{\leq a}$ is increased to $X_{\leq b}$ using the language of attachments. Moving from $X_{\leq a}$ to $X_{\leq b}$ is a homotopy equivalence (no change in topology) unless h has critical values in $[a, b]$. When there is a single critical point $\boldsymbol{z}$ with height in this interval, the topology changes via a topological attachment: $X_{\leq b}$ is homotopy equivalent to $X_{\leq a}$ on which a λ-ball B is glued via an attaching map $\phi : \partial B \to X_{\leq a}$. The value of λ is the *Morse index* of the critical point $\boldsymbol{z}$, which can be thought of as the dimension of the downward facing part of the generalized saddle at $\boldsymbol{z}$ and computed in local coordinates using the Hessian of h at $\boldsymbol{z}$.

Figure C.3 in Appendix C shows how the decapitated unit sphere $S_{\leq 1-\varepsilon}$ becomes the full unit sphere by the attachment of a cap and the north pole (Morse index 2), while Figure C.5 in Appendix C shows how a contractible patch near

https://doi.org/10.1017/9781108874144.012 Published online by Cambridge University Press

the bottom of a torus becomes homotopy equivalent to a circle when a bridge (homotopy equivalent to an arc) is added at the first Morse index-1 critical point. These diagrams are reproduced here in Figure 7.10 for convenience.

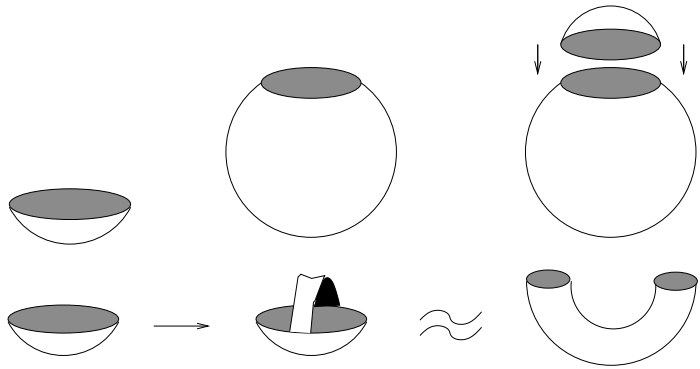

Figure 7.10 Two examples of attachments.

We now specialize to the case where $X = \mathcal{V}_*$ and $h = h_{\hat{\boldsymbol{r}}}$ for some fixed unit vector $\hat{\boldsymbol{r}}$. It is not true that h will always be proper, however we can work around this difficulty. If $\boldsymbol{\sigma} \in \mathcal{V}_*$ is a critical point then the gradient $(\nabla h_{\hat{\boldsymbol{r}}})(\boldsymbol{\sigma})$ projects to zero on the tangent plane $T_{\boldsymbol{\sigma}}\mathcal{V}_* \subset \mathbb{C}^d$. Roughly speaking, a *critical point at infinity* is a sequence of points $\boldsymbol{z}^{(k)} \in \mathcal{V}_*$ going off to infinity such that the projection of $(\nabla h_{\hat{\boldsymbol{r}}})(\boldsymbol{z}^{(k)})$ to $T_{\boldsymbol{z}^{(k)}}\mathcal{V}_*$ approaches zero as $k \to \infty$; the associated *critical value at infinity* is the limit of $h_{\hat{\boldsymbol{r}}}(\boldsymbol{z}^{(k)})$ as $k \to \infty$. Critical points at infinity are defined formally in Definition 7.42 below. Provided there are no critical points at infinity, the classic results of Morse theory hold even when the height function is not proper.

Lemma 7.14. *Suppose $h_{\hat{\boldsymbol{r}}}$ has no critical values at infinity in the interval $[a, b]$. If there are no critical values in $[a, b]$ then the inclusion $X_{\leq a} \subseteq X_{\leq b}$ is a homotopy equivalence. If there is a single critical point $\boldsymbol{z}$ with critical value $h_{\hat{\boldsymbol{r}}}(\boldsymbol{z}) = c \in (a, b)$, then the pair $(\mathcal{V}_{\leq b}, \mathcal{V}_{\leq a})$ is homotopy equivalent to a λ-cell relative to its boundary, where λ is the Morse index of the critical point $\boldsymbol{z}$ for $h_{\hat{\boldsymbol{r}}}$.*

Exercise 7.7. What is λ in the attachment in the bottom row of Figure 7.10?

It is convenient to postpone the proof of Lemma 7.14 until the more general setting when we no longer require $\mathcal{V}$ to be smooth. After establishing additional results below, Lemma 7.14 follows directly from Lemma 7.25, which asserts the homotopy equivalence, and the identification of the attachment in

https://doi.org/10.1017/9781108874144.012 Published online by Cambridge University Press

Theorem 7.35(b). In the present smooth case, a nice simplification occurs: because the height function is the real part of a complex (locally) analytic function, every critical point $\boldsymbol{z} \in \mathcal{V}_*$ has Morse index $d-1$.

Exercise 7.8. Prove that the real part of a complex analytic function defined on an open set in $\mathbb{C}^d$ has Morse index d, then prove that the real part of such a function restricted to a smooth hypersurface has Morse index $d-1$. *Hint:* The Cauchy–Riemann equations yield a lot of information about the eigenvectors and eigenvalues of the Hessian.

This characterization of the index allows us to show that $H_{d-1}(\mathcal{V}_*)$ is homologically a *bouquet of* $(d-1)$*-spheres*, one quasi-local to each critical point. A version of the following theorem, with the stronger assumption that h is proper replacing the assumption of no CVAI, is stated and proved as Theorem C.39 in Appendix C (the appendices contain background material not specialized to ACSV). The restriction that the critical values are distinct is removed in Corollary 7.17.

Theorem 7.15. *Assume that $\mathcal{V}$ is smooth, $h_{\hat{\boldsymbol{r}}}$ is a Morse height function, and there are no critical values at infinity (according to Definition 7.43 below). Assume further that the critical values $c_j = h_{\hat{\boldsymbol{r}}}(\boldsymbol{z}_j)$ are distinct and listed in descending order.*

(i) Each projection $H_{d-1}(\mathcal{V}_*) \to H_{d-1}(\mathcal{V}_{\leq c_j+\varepsilon}, \mathcal{V}_{\leq c_j-\varepsilon})$ is surjective. In other words, the relative homology generator at $\boldsymbol{z}_j$ can be chosen to be an absolute cycle.

(ii) Each inclusion $\mathcal{V}_{\leq c} \subseteq \mathcal{V}_*$ induces an injection on H_{d-1}. In other words, there are no relations: no homology generator ever gets killed.

It follows that $H_{d-1}(\mathcal{V}_*) \cong \mathbb{Z}^m$ and that a basis $\gamma_1, \ldots, \gamma_m$ for $H_{d-1}(\mathcal{V}_*)$ can be chosen so that each γ_j is a cycle on which $h_{\hat{\boldsymbol{r}}}$ attains its maximum value at $\boldsymbol{z}_j$.

Proof Part (*i*) of Theorem 7.44 below extends the fundamental Morse Lemma, namely homotopy equivalence of $\mathcal{M}_{\leq c}$ as c varies in an interval with no critical values (Lemma C.27) from the case where h is a proper Morse function to the case where h need not be proper but there are no CVAI in the interval. Part (*ii*) of Theorem 7.44 extends the smooth attachment theorem for a single critical value c (Theorem C.28) from the case where h is a proper Morse function to the case where h need not be proper but there are no CVAI in the interval. Accordingly, the conclusions of Theorems C.38 and C.39 hold for this case, via the same argument. Specifically, these follow from the identification of the attachment and from the homology long exact sequence for the filtration of pairs $(\mathcal{M}_{\leq b_j}, -\infty)$, where b_j are real numbers between each successive pair of

https://doi.org/10.1017/9781108874144.012 Published online by Cambridge University Press

critical values, b_0 is above the highest critical value, and $-\infty$ is $\mathcal{M}_b$ for any b less than the least critical value. See Section C.4 for details. □

Remark 7.16. The isomorphism $H_{d-1}(\mathcal{V}_*) \cong \bigoplus_{j=1}^m H_{d-1}(\mathcal{V}_{c_j+\varepsilon}, \mathcal{V}_{c_j-\varepsilon})$ is not natural. For each attachment at $\boldsymbol{z}_j$ there is an arbitrary choice of an absolute cycle γ_j that projects to the generator of the homology group for the attachment. The cycle $\gamma_j + \alpha$ would do equally well for any cycle α supported on $\mathcal{V}_{c_j-\varepsilon}$. One might say that the choice of $\gamma_1, \ldots, \gamma_m$, listed in decreasing order of height, can be altered by an arbitrary upper triangular map, replacing γ_j by $\gamma_j + \sum_{i>j} b_i \gamma_i$. This is the so-called ***Stokes phenomenon***, illustrated in Figure 7.11: the saddle point integral from $\boldsymbol{z}_j$ might pass on either side of $\boldsymbol{z}_i$ as it travels downward, with the integrals over the two choices of contour differing by the integral over γ_i. Thus, for a cycle C the decomposition $[C] = \sum_{k=1}^m n_k \gamma_k$ is not natural. It is important to note, however, that the leading coefficient n_{j_*} is well-defined independent of the chosen basis $\{\gamma_j\}$, where j_* is the least index such that $n_{j_*} \neq 0$.

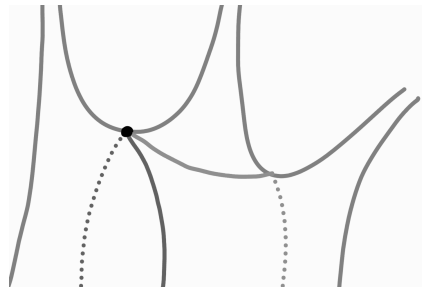

Figure 7.11 Stokes's phenomenon reflects the fact that a curve draped over the higher saddle can descend on either side of the lower saddle, as shown here by two possible branches. The difference between these two curves is a curve draped over the lower saddle.

The simplifying assumption of distinct critical values is not important. To get rid of this, we define the local homology pair $\mathcal{V}^{\boldsymbol{p},loc}$ at a critical point $\boldsymbol{p}$ at height c to be the pair (X, Y), where $Y = \mathcal{V}_{\leq c-\varepsilon/2}$ and X is the union of Y with the ball $B_\varepsilon(\boldsymbol{p})$ for $\varepsilon > 0$ sufficiently small (see Definition C.31 of Appendix C for full details). Any such pairs are homotopy equivalent as long as ε is small enough that the 2ε-balls about different critical points are disjoint.

Deformations defined in Appendix C show that if there is a unique critical point $\boldsymbol{p}$ with height $c \in [a, b]$ then, for small $\varepsilon > 0$, the local pair $\mathcal{V}^{\boldsymbol{p},loc}$ is homotopy equivalent to the *slab* $(\mathcal{V}_{\leq c+\varepsilon}, \mathcal{V}_{c-\varepsilon})$. The benefit to replacing the slab by the local pair occurs when there are multiple critical points sharing a

https://doi.org/10.1017/9781108874144.012 Published online by Cambridge University Press

critical value. If $h_{\hat{\boldsymbol{r}}}(\boldsymbol{p}) = c$ for all $\boldsymbol{p}$ in some finite set E then

$$(\mathcal{V}_{\le b}, \mathcal{V}_{\le a}) \simeq \bigoplus_{\boldsymbol{p}\in E} \mathcal{V}^{\boldsymbol{p},\mathrm{loc}}, \tag{C.3.1}$$

giving the following.

Corollary 7.17. *Replacing* $(\mathcal{V}_{c_j+\varepsilon}, \mathcal{V}_{c_j-\varepsilon})$ *by* $\mathcal{V}^{\boldsymbol{z},\mathrm{loc}}$ *for each* $\boldsymbol{z}$*, the conclusions of Theorem 7.15 hold without the assumption of distinct critical values.* □

We end this subsection with some examples of this topological decomposition.

Example 7.18 (binomial coefficients)**.** Recall that the binomial coefficients $a_{rs} = \binom{r+s}{r}$ have bivariate generating function $F(x, y) = 1/(1-x-y)$. If $\hat{\boldsymbol{r}} = (r, s)$ with $r + s = 1$ and $r, s \in (0, 1)$ then as r varies from 0 to 1, the critical point $\boldsymbol{w}(\hat{\boldsymbol{r}})$ of F in the direction $\hat{\boldsymbol{r}}$ slides from $(0, 1)$ to $(1, 0)$. The homology group $H_1(\mathcal{V}_*)$ has a single generator $\gamma_{\boldsymbol{z}_*}$. The homology group $H_2(\mathcal{M})$ is cyclic as well, generated by $\mathsf{o}\gamma_{\boldsymbol{z}_*}$. ◁

Example 7.19 (Delannoy numbers)**.** The Delannoy number generating function from Example 2.7 in Chapter 2 is $1/(1-x-y-xy)$. The situation is similar to Example 7.18, except that as r varies from 0 to 1 the critical point $\boldsymbol{w}(\hat{\boldsymbol{r}})$ traverses the arc the other way from $(0, 1)$ to $(1, 0)$, and there is another critical point $\boldsymbol{w}'$ traversing a hyperbola in the third quadrant. ◁

Exercise 7.9. Consider the amoeba of the denominator $Q(x, y) = 1 - x - y - xy$ of the Delannoy generating function, shown in Figure 7.12.

(a) Compute the critical points $\boldsymbol{w}$ and $\boldsymbol{w}'$ in the direction determined by $\boldsymbol{r} = (2, 3)$, then draw dots where $\boldsymbol{p} = \mathrm{Relog}(\boldsymbol{w})$ and $\boldsymbol{p}' = \mathrm{Relog}(\boldsymbol{w}')$ lie on the amoeba.

(b) Find a path β, from the power series component of the amoeba complement to a component where the Cauchy integral is zero, that enters the amoeba at $\boldsymbol{p}$ and exits it at $\boldsymbol{p}'$.

(c) Describe $\gamma = \mathrm{Relog}^{-1}(\beta)$.

(d) State why $[\gamma] = \mathbf{INT}(T, T')$ in $H_1(\mathcal{V}_*)$ and why $\int_\gamma \mathrm{Res}\,\omega$ is easy to estimate, where

$$\omega = \frac{x^{-2n-1}y^{-3n-1}}{1 - x - y - xy}\,dx \wedge dy\,.$$

https://doi.org/10.1017/9781108874144.012 Published online by Cambridge University Press

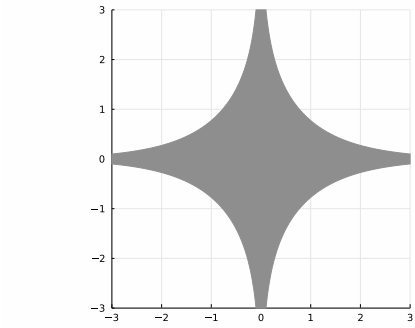

Figure 7.12 Amoeba for the Delannoy generating function $Q(x, y) = 1 - x - y - xy$. Each point interior to the amoeba is the image of precisely two points of $\mathcal{V}$ under Relog.

Result: a saddle point integral decomposition in the smooth case

Theorem 7.15 and Corollary 7.17 give a basis of $H_{d-1}(\mathcal{V}_*)$ consisting of cycles that attain their maximum values at critical points. Vanishing of $dh_{\hat{\boldsymbol{r}}}|_{\mathcal{V}}$ at $\boldsymbol{z}$ is equivalent to $\boldsymbol{z}^{-\boldsymbol{r}}$ being in stationary phase at $\boldsymbol{z}$ for any $(d-1)$-chain γ_j supported on $\mathcal{V}_*$. Thus, combining Theorem 7.15 and Corollary 7.17 with the integral representation in Proposition 7.13 gives the following, our ultimate goal for generating functions with smooth singular varieties.

Theorem 7.20 (smooth saddle point integral decomposition)**.** *Assume that $\mathcal{V}$ is smooth, $h_{\hat{\boldsymbol{r}}}$ is a Morse height function, and that there are no critical values at infinity (see Definition 7.43 below). Assume further that the critical values $c_j = h_{\hat{\boldsymbol{r}}}(\boldsymbol{z}_j)$ for $1 \leq j \leq m$ are listed in descending order. Then there exist integers $\kappa_j \in \mathbb{Z}$ and smooth chains of integration γ_j with heights uniquely maximized at $\boldsymbol{z}_j$, such that*

$$a_{\boldsymbol{r}} = \sum_{j=1}^{m} \frac{\kappa_j}{(2\pi i)^{d-1}} \int_{\gamma_j} \boldsymbol{z}^{-\boldsymbol{r}-\mathbf{1}} \operatorname{Res}(F(\boldsymbol{z})\, d\boldsymbol{z})\,. \tag{7.11}$$

The integral in the jth summand is in stationary phase at $\boldsymbol{z}_j$. The least j such that $\kappa_j \neq 0$, and the homology class $\sum_{j' \in E} \kappa_{j'} \gamma_{j'}$ for all j' such that $\boldsymbol{z}_{j'}$ has height c_j, are uniquely defined. □

There are two important tasks remaining: computing asymptotics of the saddle point integrals and determining the integers κ_j. While integral asymptotics (in this smooth case) follow in a straightforward manner from the results of Chapter 5, it can be very difficult to determine these unknown integers. We

https://doi.org/10.1017/9781108874144.012 Published online by Cambridge University Press

discuss both of these questions in Chapter 9, where we derive explicit asymptotic formulae for a_r in terms of the generating function $F(z)$. Readers who are interested only in smooth asymptotics (and do not need to see the technical discussion of critical points at infinity) may go directly to Chapters 8 and 9, after a brief discussion about removing our simplifying hypotheses.

The requirement of no critical value at infinity is essential: when there are critical points at infinity, asymptotics are in principle affected. Classifying these cases and computing the asymptotics remains an open problem discussed further in Chapter 13. Removing the smoothness assumption involves the apparatus of stratified Morse theory, which we make use of in the next section. The assumption that $h_{\hat{r}}$ is nondegenerate is not essential, however in its absence there is no longer a unique cycle γ_j for each j. We handle this case, for now, by two examples.

Example 7.21 (cubic degeneracy)**.** The simplest degeneracy at a critical point, a so-called *monkey saddle*, leads to two independent homology generators as in Figure 7.13. ◁

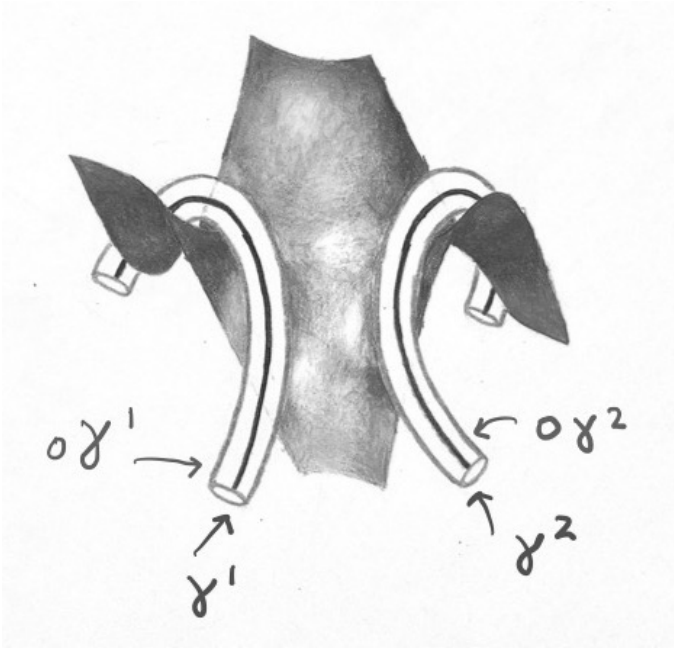

Figure 7.13 Two homology generators associated with a monkey saddle.

https://doi.org/10.1017/9781108874144.012 Published online by Cambridge University Press

While critical points are generically nondegenerate, we now give one combinatorial example in which a critical point $\boldsymbol{w}$ is indeed degenerate and contributes more than one generator.

Example 7.22 (bi-colored supertrees)**.** Example 9.32 in Chapter 9 looks at a rational generating function counting bi-colored supertrees (certain planar binary trees that need not concern us here). The singular variety is the smooth surface defined by the vanishing of $Q(x, y) = x^5y^2 + 2x^2y - 2x^3y + 4y + x - 2$. When $\hat{\boldsymbol{r}} = (1/2, 1/2)$ then there are two nondegenerate critical points, $\mathbf{u}$ and $\mathbf{v}$, together with a critical point $\boldsymbol{w}$ near which $h_{\hat{\boldsymbol{r}}}$ is quartic (so doubly degenerate). Accordingly there is one cycle $\gamma_{\mathbf{u}}$, one cycle $\gamma_{\mathbf{v}}$, and three cycles $\gamma_{\boldsymbol{w}}^{(j)}$ which may be configured all to enter $\boldsymbol{w}$ along the solid arc and exit along one of the three dashed arcs shown in Figure 7.14. ◁

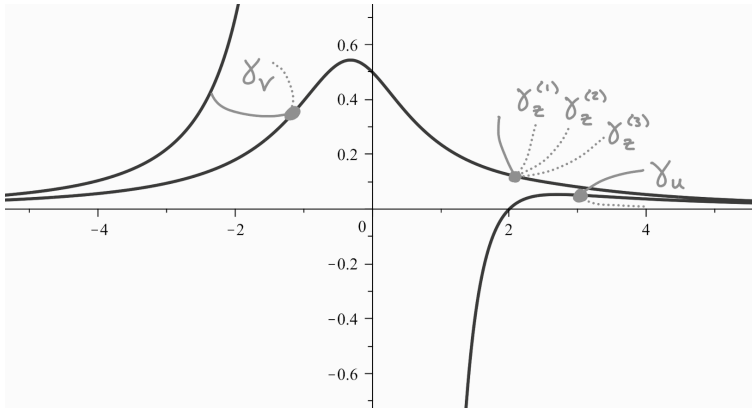

Figure 7.14 The supertree generating function yields two nondegenerate critical points and one doubly degenerate critical point.

7.3 The general case via stratified Morse theory

We now drop the assumption that the singular variety $\mathcal{V}$ is smooth. As detailed in Appendix D, the correct notion for us is the concept of a *Whitney stratified space*: every real or complex algebraic (or analytic) variety admits a *Whitney stratification*, and the analytic constructions we require for asymptotics can be built for stratified spaces. In this chapter we recount only the results from Appendix D that we directly require. Although we typically assume that F is

https://doi.org/10.1017/9781108874144.012 Published online by Cambridge University Press

a rational function to simplify our presentation, the results discussed here hold for general meromorphic functions with minor modifications.

Example 7.23. Figure 7.15 shows the zero set $\mathcal{V}$ of the polynomial $Q = (z^3 - x^2)(2 - x - y - z)$. We can split the variety $\mathcal{V}$ into a finite number of semi-algebraic strata (defined by polynomial equalities and inequalities): two strata of codimension 1,

$$S_1 = \left\{x + y + z = 2 \text{ and } z^3 - x^2 \neq 0\right\}$$
$$S_2 = \left\{z^3 - x^2 = 0 \text{ and } x + y + z \neq 2\right\} \setminus \{x = z = 0\},$$

two strata of codimension 2,

$$S_3 = \left\{z^3 - x^2 = 0 \text{ and } x + y + z = 2 \text{ and } (x, z) \neq (0, 0)\right\},$$
$$S_4 = \{(x, z) = 0 \text{ and } y \neq 2\},$$

and one stratum of codimension 3 at the point

$$S_5 = \{z^3 - x^2 = x + y + z - 2 = x = z = 0\} = \{(0, 2, 0)\}.$$

Note that we introduce additional strata both to account for multiple irreducible components of $\mathcal{V}$ and to account for singularities in individual components. ◁

As described in Appendix D, it is usually not sufficient to partition $\mathcal{V}$ into any general set of smooth manifolds – we must also make sure the elements in such a partition "fit together nicely." This concept is formalized by the notion of a Whitney stratification, given in Definition D.3 of Appendix D. For the rest of this chapter we fix a Whitney stratification of $\mathcal{V}$, which is a partition of $\mathcal{V}$ into manifolds $\{S_\alpha : \alpha \in I\}$ indexed by some partially ordered set I such that

(i) $S_\alpha \cap \overline{S_\beta} \neq \emptyset$ if and only if $S_\alpha \subset \overline{S_\beta}$ if and only if $\alpha \leq \beta$, and
(ii) if $\alpha < \beta$, if the sequences $\{x_i \in S_\beta\}$ and $\{y_i \in S_\alpha\}$ both converge to $y \in S_\alpha$, if the lines $\ell_i = \overline{x_i y_i}$ converge to a line ℓ, and if tangent planes $T_{x_i}(S_\beta)$ converge to a plane T, then both ℓ and $T_y(S_\alpha)$ are contained in T.

We always take *algebraic* stratifications defined by polynomial equalities and inequalities. In fact, we may assume that our Whitney stratification is defined by a finite sequence of nested algebraic sets $\mathcal{V} = F_0 \supset F_1 \supset \cdots \supset F_m = \emptyset$ such that the connected components of the sets $F_i \setminus F_{i+1}$ for all $1 \leq i \leq m-1$ form the strata. If S is a stratum defined as a connected component of $F_i \setminus F_{i+1}$ then the ***dimension of the stratum*** S (respectively the ***codimension of the stratum*** S) is the dimension (respectively codimension) of $F_i \subset \mathbb{C}^d$ as an algebraic set. Whitney stratifications exist for all algebraic (and analytic) varieties, and algorithms to compute them are discussed in Chapter 8 and Appendix D.

https://doi.org/10.1017/9781108874144.012 Published online by Cambridge University Press

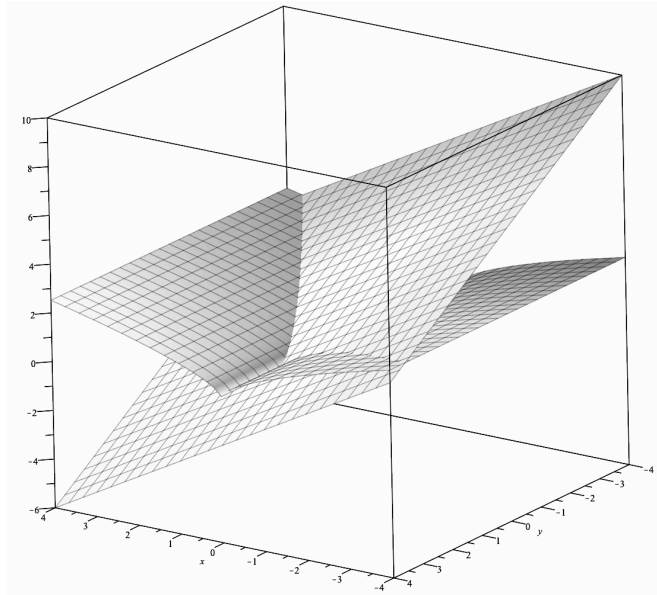

Figure 7.15 The zero set of $Q = (z^3 - x^2)(2 - x - y - z)$.

Stratified critical points

A point $\boldsymbol{p}$ in a stratum S is said to be a ***(stratified) critical point*** for the height function $h = h_{\hat{\boldsymbol{r}}}$ if the restriction $dh|_S$ vanishes at $\boldsymbol{p}$. Analogously to the smooth case above, because h is the real part of $\phi(\boldsymbol{z}) = -\boldsymbol{r} \cdot \log \boldsymbol{z}$ the Cauchy–Riemann equations imply that $\boldsymbol{p}$ is a critical point if the gradient of ϕ lies in the normal space to S at $\boldsymbol{p}$. If S has codimension k then there exists an open set $U \subset \mathbb{C}^d$ containing $\boldsymbol{p}$ and irreducible polynomials $g_1, \ldots, g_k$ such that $S \cap U = \mathcal{V}(g_1, \ldots, g_k) \cap U$ (i.e., S is locally defined by the polynomials g_i near $\boldsymbol{p}$). The point $\boldsymbol{p}$ is a critical point if and only if the gradient $(\nabla\phi)(\boldsymbol{p})$ lies in the complex span of the gradients $(\nabla g_1)(\boldsymbol{p}), \ldots, (\nabla g_k)(\boldsymbol{p})$. Although ϕ involves logarithms, its gradient is a rational function, so we may compute stratified critical point by solving polynomial systems. Computation of stratified critical points is discussed at greater length in Chapter 8.

Recall from Chapter 6 that the *logarithmic gradient* of a differentiable function f at $\boldsymbol{z} \in \mathbb{C}^d$ is the vector

$$\nabla_{\log} f(\boldsymbol{z}) = (z_1 f_{z_1}, \ldots, z_d f_{z_d}(\boldsymbol{z})) \,, \tag{7.12}$$

with the word *logarithmic* coming from the fact that the logarithmic gradient of $f(\boldsymbol{z})$ at $\boldsymbol{z} = \exp(\boldsymbol{x})$ is the gradient of $(f \circ \exp)(\boldsymbol{z})$ at $\boldsymbol{z} = \boldsymbol{x}$. If $\boldsymbol{p}$ is a smooth

https://doi.org/10.1017/9781108874144.012 Published online by Cambridge University Press

point of the algebraic hypersurface defined by the vanishing of Q, then the vanishing of $dh_{\hat{\boldsymbol{r}}}|_{\mathcal{V}}$ at $\boldsymbol{p}$ is equivalent to the direction vector $\hat{\boldsymbol{r}}$ being parallel to $(\nabla_{\log} Q)(\boldsymbol{p})$. More generally, vanishing of $dh_{\hat{\boldsymbol{r}}}|_S$ at $\boldsymbol{p}$ is equivalent to $\hat{\boldsymbol{r}}$ lying in the space spanned by the logarithmic gradients of the functions g_j locally defining the stratum S at $\boldsymbol{p}$.

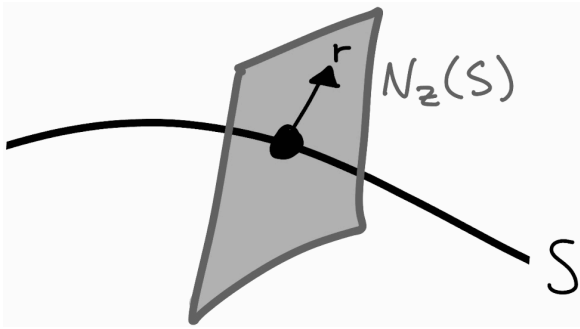

Figure 7.16 The point $\boldsymbol{z}$ on a stratum S defined by the vanishing of two transversely intersecting smooth sheets in three dimensions is a critical point in the direction $\hat{\boldsymbol{r}}$ if $\boldsymbol{r}$ lies in the log-normal plane to S at $\boldsymbol{z}$.

Example 7.24. If $\mathcal{V}$ is the union of two transversely intersecting smooth sheets defined by the vanishing of two polynomials g_1 and g_2 then $\boldsymbol{z}$ is a critical point on $\mathcal{V}_{g_1} \setminus \mathcal{V}_{g_2}$ in a direction $\hat{\boldsymbol{r}}$ if $\boldsymbol{r}$ is parallel to $(\nabla_{\log} g_1)(\boldsymbol{z})$, and the analogous criteria holds for critical points on $\mathcal{V}_{g_2} \setminus \mathcal{V}_{g_1}$. A critical point $\boldsymbol{z}$ on the intersection stratum $S = \mathcal{V}_{g_1} \cap \mathcal{V}_{g_2}$, pictured in Figure 7.16, has $\boldsymbol{r}$ lying somewhere in the log-normal plane spanned by $(\nabla_{\log} g_1)(\boldsymbol{z})$ and $(\nabla_{\log} g_2)(\boldsymbol{z})$. ◁

Exercise 7.10. Describe the set of directions $\boldsymbol{r} \in \mathbb{R}^2_*$ such that $dh_{\hat{\boldsymbol{r}}}|_S = 0$ at a point (x, y, z) of the codimension 2 stratum S_3 in Example 7.23.

Obstructions are critical points

The fundamental lemma of Morse theory, described in Lemma 7.14 above, states that, in the absence of critical values at infinity, critical values are the only places the topology of the sublevel sets of a manifold can change. The fundamental lemma of *stratified* Morse theory says that (stratified) critical values are still the only places the topology of $\mathcal{M}_{\leq c}$ and $\mathcal{V}_{\leq c}$ can change, and thus are the only places obstructions to pushing down cycles of integration can occur. Lemma 7.14 also specifies the nature of the attachment at a critical point, but since this requires a more lengthy explanation, we state the stratified version of Lemma 7.14 without describing the attachment. As a reminder, we

https://doi.org/10.1017/9781108874144.012 Published online by Cambridge University Press

postpone the formal definitions of critical points at infinity and critical values at infinity until Definition 7.42 below.

Lemma 7.25. *If $h_{\hat{\boldsymbol{r}}}$ has no critical values (including at infinity) in $[a, b]$, then the inclusion $\mathcal{M}_{\leq a} \subseteq \mathcal{M}_{\leq b}$ is a homotopy equivalence. The same is true of the inclusion $\mathcal{V}_{\leq a} \subseteq \mathcal{V}_{\leq b}$.*

Remark 7.26. The fact that stratified critical values isolate all the topological change in $\mathcal{V}_*$ may be less surprising than the fact that they do so in $\mathcal{M}$.

Let $\boldsymbol{p}$ be a stratified critical point for $h_{\hat{\boldsymbol{r}}}$ in some stratum S. Mirroring our definition of $\mathcal{V}^{\boldsymbol{p},\mathrm{loc}}$ above, we let

$$\mathcal{M}^{\boldsymbol{p},\mathrm{loc}} := (\mathcal{M}_{\leq c-\varepsilon} \cup B_{2\varepsilon}(\boldsymbol{p}), \mathcal{M}_{\leq c-\varepsilon}),$$

for any sufficiently small $\varepsilon > 0$, which is defined up to homotopy equivalence.

The simplifying assumption of distinct critical values often fails in ACSV, for example if there is a pair of complex conjugate critical points, necessitating one further definition. Let c be a critical value, let $\boldsymbol{p}_1, \ldots, \boldsymbol{p}_m$ be the critical points at height c, and assume ε is sufficiently small so that the balls $B_{2\varepsilon}(\boldsymbol{p}_i)$ are disjoint.

Definition 7.27 (all attachments at height c)**.** Under the setup above, the ***total attachment pair*** at height c is

$$(\mathcal{M}_{c+}, \mathcal{M}_{c-}) := \left(\mathcal{M}_{\leq c-\varepsilon} \cup \bigcup_{j=1}^{m} B_{2\varepsilon}(\boldsymbol{p}_j), M_{\leq c-\varepsilon} \right). \tag{7.13}$$

By disjointness of the balls $B_{2\varepsilon}(\boldsymbol{p}_j)$, this is a direct sum in the category of pairs of $\mathcal{M}^{\boldsymbol{p}_j,\mathrm{loc}}$, hence the homology $H_*(\mathcal{M}_{c+}, \mathcal{M}_{c-})$ is the direct sum $\bigoplus_{j=1}^{m} H_*(\mathcal{M}^{\boldsymbol{p}_j,\mathrm{loc}})$.

Lemma 7.28. *Suppose $h_{\hat{\boldsymbol{r}}}$ has no critical values at infinity in $[a, b]$ and has a single critical value c in $[a, b]$, occurring in the interior (a, b). Then the pairs $(\mathcal{M}_{\leq b'}, \mathcal{M}_{\leq a'})$ are naturally homotopy equivalent for any $a \leq a' < c < b' \leq b$.*

Lemmas 7.25 and 7.28 are taken from [BMP22]; a sketch of the proof is reproduced in Section 7.5.

Building by attachment

We now fit together the attachments at critical points of all possible heights. This involves classical topological facts, and works without knowing the homotopy type of any individual attachment.

Let $c_1 > c_2 > \cdots > c_m$ denote the critical values in the interval $[c_m, \infty)$

https://doi.org/10.1017/9781108874144.012 Published online by Cambridge University Press

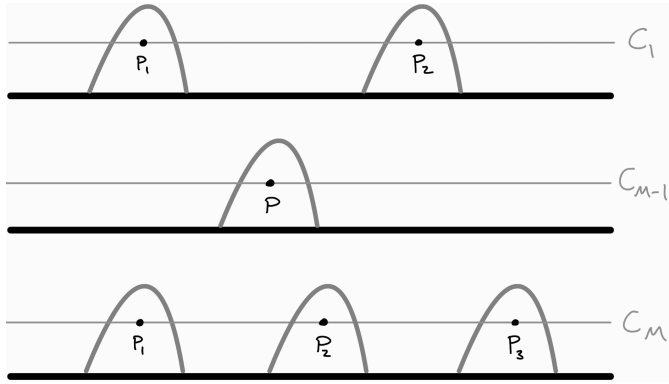

Figure 7.17 Building $\mathcal{M}$ via successive attachments at the critical values $c_1 > c_2 > \cdots > c_m$. In this case we attach three bumps to $\mathcal{M}_{c_m-}$ around critical points at height c_m, then attach a single bump, and so on until attaching two final bumps.

and assume there are no CVAI in $[c_m, \infty)$. For each j let c_{j-} denote $c_j - \varepsilon$ where $\varepsilon > 0$ is sufficiently small so that there are no critical values or CVAI in $[c_j - \varepsilon, c_j)$, and let c_{j+} denote $c_j + \varepsilon$ where $\varepsilon > 0$ is sufficiently small so that there are no critical values or CVAI in $(c, c_j + \varepsilon]$. Intuitively, we think of building up the space $\mathcal{M}$ from the space $\mathcal{M}_{c_m-}$ by successive attachment. First, we attach $(\mathcal{M}_{c_m+}, \mathcal{M}_{c_m-})$ to arrive at the space $\mathcal{M}_{c_m+}$, which, by Lemma 7.28, is homotopy equivalent to the space $\mathcal{M}_{c_{m-1}-}$. Next we attach the pair $(\mathcal{M}_{c_{m-1}+}, \mathcal{M}_{c_{m-1}-})$. Repeating this until the pair $(\mathcal{M}_{c_1+}, \mathcal{M}_{c_1-})$ has been attached, we have built the space $\mathcal{M}_{c_1+}$, which is homotopy equivalent to $\mathcal{M}_{\leq b}$ for all sufficiently large b, and hence to $\mathcal{M}$ itself. This process is illustrated in Figure 7.17. The "bump" $\mathcal{N}(\boldsymbol{p})$ near a point $\boldsymbol{p}$ is the intersection of $\mathcal{M}$ with a ball of sufficiently small radius δ. Shrinking ε if necessary, $(\mathcal{M}_{c_j-} \cup \mathcal{N}(\boldsymbol{p}), \mathcal{M}_{c_j})$ has the homotopy type of the local pair $\mathcal{M}^{\boldsymbol{p},\mathrm{loc}}$ discussed above.

Each attachment has a long exact homology sequence. Because all of the spaces involved are cell complexes of real dimension at most d (see Section D.4 of Appendix D), the homology groups H_k of dimension $k \geq d+1$ vanish. Thus, the long exact sequence for any $j \leq m$ always begins

$$0 \to H_d(\mathcal{M}_{c_j-}) \to H_d(\mathcal{M}_{c_j+}) \to H_d(\mathcal{M}_{c_j+}, \mathcal{M}_{c_j-}) \to \cdots . \tag{7.14}$$

Definition 7.29. For each critical point $\boldsymbol{p}$ at height c_j, let $G(\boldsymbol{p})$ denote the image in $H_d(\mathcal{M}_{c_j+}, \mathcal{M}_{c_j-})$ of the map projecting $\mathcal{M}_{c_j-} \cup \mathcal{N}(\boldsymbol{p})$ to the pair $(\mathcal{M}_{c_j-} \cup \mathcal{N}(\boldsymbol{p}), \mathcal{M}_{c_j})$, as in Figure 7.17. In other words, $G(\boldsymbol{p})$ are those relative d-homology classes, once the bump $\mathcal{N}(\boldsymbol{p})$ near $\boldsymbol{p}$ is added, that are represented by absolute cycles. We further define $G = G(c_j) := \bigoplus_{h(\boldsymbol{p})=c_j} G(\boldsymbol{p})$.

https://doi.org/10.1017/9781108874144.012 Published online by Cambridge University Press

The sequence (7.14) gives rise to the short exact sequence

$$0 \to H_d(\mathcal{M}_{c_j-}) \to H_d(\mathcal{M}_{c_j+}) \to G \to 0\,. \tag{7.15}$$

As we are working with coefficients in $\mathbb{C}$, there is no torsion, hence the short exact sequence implies a (not natural) direct sum

$$H_d(\mathcal{M}_{c_j+}) \cong H_d(\mathcal{M}_{c_j-}) \oplus H_d(\mathcal{M}_{c_j+}, \mathcal{M}_{c_j-})\,. \tag{7.16}$$

Assuming Lemmas 7.25 and 7.28, we have proved the following.

Theorem 7.30. *Suppose there are no critical values at infinity above height a and finitely many critical values $c_1 > \cdots > c_m$ in $[a, \infty)$. Then the homology of $\mathcal{M}$ is given by*

$$H_d(\mathcal{M}) \cong H_d\left(\mathcal{M}_{<a}\right) \oplus \bigoplus_{\boldsymbol{p}} G(\boldsymbol{p})\,,$$

where $G(\boldsymbol{p})$ is defined in Definition 7.29 and the sum is over critical points $\boldsymbol{p}$ such that $h_{\hat{\boldsymbol{r}}}(\boldsymbol{p}) \geq a$. If there are no critical values at infinity and finitely many critical values then

$$H_d(\mathcal{M}, \mathcal{M}_{-\infty}) \cong \bigoplus_{\boldsymbol{p}} G(\boldsymbol{p})$$

where $M_{-\infty}$ denotes $\mathcal{M}_{\leq a}$ for any a less than the least critical value, and the sum is over all critical points. □

Description of the attachments

Next we describe the attachment cycles for $\mathcal{M}$. We could also develop the attachment cycles for $\mathcal{V}_*$ in the stratified setting, however our asymptotic results don't need them so we skip this extra step.

The key to understanding attachments in Whitney stratified spaces is a local product structure described in Theorem D.9 of Appendix D, which follows from the famous (and somewhat difficult) Thom's Isotopy Lemma (Lemma D.16 in Appendix D). The Isotopy Lemma says that for a fixed stratum S of dimension j and any point $\boldsymbol{p} \in S$ there is a neighborhood of $\boldsymbol{p}$ where the space $\mathcal{V}$ looks like $\mathbb{R}^j \times N$ where N is the *normal slice* of the strata (see Definition 7.32 and Figure 7.18 below).

What does the local product structure imply for our attachments? Let $\boldsymbol{p} \in S$ be a critical point for the height function h, and consider S as a complex manifold of dimension i (where it has dimension $j = 2i$ as a real manifold). Because h is the real part of (a branch of) an analytic function, it is harmonic and all critical points have Morse index i. Thus, when S is arranged by height near $\boldsymbol{p}$ there is an i-dimensional part that 'bends downwards' and an i-dimensional

https://doi.org/10.1017/9781108874144.012 Published online by Cambridge University Press

part that 'bends upwards'. By the local product structure, the pair for the attachment of $\mathcal{M}$ at $\boldsymbol{p}$ is (homotopy equivalent to) the product of a pair $(B^i, \partial B^i)$ in the tangent space to S and a pair $(\mathcal{L}, \mathcal{L} \cap \mathcal{M}_{\leq c-\varepsilon})$, where c is the height of $\boldsymbol{p}$, the constant $\varepsilon > 0$ is sufficiently small, and $\mathcal{L}$ denotes the *normal link* (the intersection of $\mathcal{M}$ with the normal space to S at $\boldsymbol{p}$ in a suitable small neighborhood of $\boldsymbol{p}$, described in Definition 7.32 below).

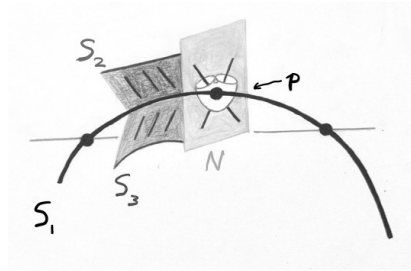

Figure 7.18 An example of an attachment given by the product of a torus with an arc (a relative 3-torus).

Example 7.31. Figure 7.18 shows an example of an attachment on a stratum S_1 with complex dimension 1 defined by the intersection of two transversely intersecting smooth sheets. In one direction it curves down, as shown; in the other direction it curves up (this is not shown). The level set defined by $h(z) = c - \varepsilon$ is the horizontal line and the pair $(B^1, \partial B^1)$ is the black arc modulo its endpoints. The normal link is the complement of two intersecting complex lines in complex 2-space, which is homotopy equivalent to a 2-torus. The 2-torus can be drawn arbitrarily close to $\boldsymbol{p}$, so it can be chosen as an absolute cycle and the pair $(\mathcal{L}, \mathcal{L} \cap \mathcal{M}_{\leq c-\varepsilon})$ is simply $(\mathcal{L}, \emptyset) \simeq \mathcal{L}$. The attachment pair is obtained by sliding the 2-torus along the black arc from one endpoint to the other, with the second element in the pair being the starting and ending positions. Because an arc modulo its boundary is a circle, this means the attachment is a 3-torus, manifested as a 2-torus times an arc that localizes to a 1-torus. ◁

Formal statement of the attachments

The following definitions and results are special cases of material in Section D.3 of Appendix D. Attachments are defined in the category of (homotopy types of) topological pairs, as are both the tangential and normal Morse data. Products in this category are defined by

$$(A, B) \times (C, D) = (A \times C, A \times D \cup B \times C)\,, \tag{7.17}$$

https://doi.org/10.1017/9781108874144.012 Published online by Cambridge University Press

and the homology of a product obeys the usual Künneth formula for homology with complex coefficients,

$$H_k(U \times V) = \bigoplus_{j=0}^{k} H_j(U) \times H_{k-j}(V)\,. \tag{7.18}$$

For the space $\mathcal{M}$, we define the Morse data for the attachment at a critical point $\boldsymbol{p} \in \mathcal{V}_*$ by the following steps.

Definition 7.32 (Morse data)**.** Let S be a stratum of complex codimension k containing a critical point $\boldsymbol{p}$ at height c.

(i) The *tangential Morse data* $T(\boldsymbol{p})$ at $\boldsymbol{p}$ is the homotopy type of the pair $(B^{d-k}, \partial B^{d-k})$ consisting of a ball of codimension k modulo its boundary. A representative of this class is the *unstable manifold* for the negative gradient flow induced by $h_{\hat{\boldsymbol{r}}}$ on $\mathcal{V}$ (the set of points that flow into the critical point under the positive gradient flow, see [HPS77, Section 4] or [Con78a]).

(ii) The *normal plane* $N_{\boldsymbol{p}}(\mathcal{S})$ to $\mathcal{S}$ at $\boldsymbol{p}$ is the (complex) orthogonal complement of the tangent space $T_{\boldsymbol{p}}(\mathcal{S})$.

(iii) The *normal slice* $\mathtt{N}$ at $\boldsymbol{p}$ is the mutual intersection of $\mathcal{V}$, a sufficiently small ball about $\boldsymbol{p}$, and the normal plane $N_{\boldsymbol{p}}(\mathcal{S})$.

(iv) The *normal link* $\mathcal{L}(\boldsymbol{p})$ is the mutual intersection of $\mathcal{M}$, a sufficiently small ball about $\boldsymbol{p}$, and $\mathtt{N}$.

(v) The *normal Morse data* $L(\boldsymbol{p})$ is the pair $(\mathcal{L}(\boldsymbol{p})_{\geq c}, \mathcal{L}(\boldsymbol{p})_{=c})$, where $\mathcal{L}(\boldsymbol{p})_{=c}$ is the intersection of the normal link with the real codimension 1 surface where $h_{\hat{\boldsymbol{r}}}(\boldsymbol{z}) = c$.

(vi) The *Morse data* at $\boldsymbol{p}$ is the product of the tangential and normal Morse data.

The following result, which is the main result in the monograph [GM88], is stated as Theorem D.21 in Appendix D.

Theorem 7.33. *The homotopy type of the attachment pair* $\mathcal{M}^{\boldsymbol{p},\mathrm{loc}}$ *is the Morse data at* $\boldsymbol{p}$*.* □

Theorem 7.33 yields a general topological decomposition of $H_d(\mathcal{M}, -\infty)$, which is a stratified version of Theorem 7.15.

Definition 7.34. A critical point $\boldsymbol{p}$ in direction $\hat{\boldsymbol{r}}$ on a stratum $\mathcal{S}$ is called a ***nondegenerate critical point on*** $\mathcal{S}$ if $h_{\hat{\boldsymbol{r}}}|_{\mathcal{S}}$ is nondegenerate in the sense of Definition 7.11 (meaning the Hessian for $h_{\hat{\boldsymbol{r}}}|_{\mathcal{S}}$ in local coordinates around $\boldsymbol{p}$ is nonsingular).

https://doi.org/10.1017/9781108874144.012 Published online by Cambridge University Press

Theorem 7.35. *Fix $\hat{\mathbf{r}}$ and assume there are no critical values at infinity. Let $\mathbf{z}_1, \ldots, \mathbf{z}_m$ enumerate the stratified critical points of $\mathcal{V}_*$ in (weakly) decreasing order of the height function $h_{\hat{\mathbf{r}}}$, where the stratum containing $\mathbf{z}_j$ has complex codimension k_j. If all critical points are quadratically nondegenerate then there are cycles $\gamma_1, \ldots, \gamma_m$ on $\mathcal{V}_*$, along with a basis $\beta_{j,1}, \ldots \beta_{j,s_j}$ for the k_j-homology of the normal Morse data, with the following properties.*

(a) $h_{\hat{\mathbf{r}}}$ achieves its maximum on γ_j at $\mathbf{z}_j$;
(b) $\gamma_j \simeq (B^{d-k_j}, \partial B^{d-k_j})$;
(c) A basis for the integer homology group $H_d(\mathcal{M}, -\infty)$ can be formed by cycles $\sigma_{j,i} = \gamma_j \times \beta_{j,i}$ which, for fixed j, form a basis for $G(\mathbf{z}_j)$.

Proof Theorem 7.33 and part (*i*) of Definition 7.32 imply (*a*) and (*b*). Comparing parts (*v*) and (*vi*) of the definition with Theorem 7.30 gives (*c*). The fact that $\{\sigma_{j,i}\}$ is an integer homology basis follows from the lack of torsion in $H_d(\mathcal{M})$, which follows from the fact that $\mathcal{V}_*$ and $\mathcal{M}$ have the homotopy type of a d-dimensional cell complex (see Theorem D.23), with no boundaries in dimension d. Because the Morse theoretic results identify the homotopy type of the attachments, not just the relative homology groups, the cycles $\sigma_{j,i}$ generate homology with both integer and rational coefficients. □

While this theorem may look somewhat abstract, its power lies in its generality, and typical applications can be simple. For instance, in Figure 7.19 we have a surface $\mathcal{V}$ with complement $\mathcal{M} := \mathbb{C}^2_* \setminus \mathcal{V}$ where $H_2(\mathcal{M})$ has one generator local to a critical point in a stratum of complex dimension 0 and two quasi-local to critical points in strata of dimension 1; the former has a 2-torus for its normal link, while the latter have normal links of dimension 1 which may be taken to be topological circles.

A further generalization removes the assumption of quadratic nondegeneracy. We do not use this generalization in this text, as we directly compute integral manipulations for the few quadratically degenerate cases that arise.

Corollary 7.36. *Without the assumption of quadratic nondegeneracy of $h_{\hat{\mathbf{r}}}$ at each critical point $\mathbf{p}$, a modified version of Theorem 7.35 still holds. Instead of a pair $(B, \partial B)$ consisting of a ball and its boundary, the tangential Morse data is replaced by a more general collection of $(d - k_j)$-cycles $\{\gamma_{j,k} : 1 \le k \le r_j\}$ where r_j is the rank of $H_{d-k_j}(\mathcal{V}_{\le c}, \mathcal{V}_{\le c-\varepsilon})$. Consequently, the basis in part (d) of Theorem 7.35 is instead formed by cycles $\gamma_{j,k} \times \beta_{j,i}$ for $1 \le j \le m$ with $1 \le k \le r_j$ and $1 \le i \le s_j$.*

Exercise 7.11. Let $\mathcal{M}$ be a manifold of real dimension d in $\mathbb{R}^n$ for $d < n$. Many classical Morse-theoretic analyses use the height function $h(\boldsymbol{x}) = d(\boldsymbol{p}, \boldsymbol{x})$,

https://doi.org/10.1017/9781108874144.012 Published online by Cambridge University Press

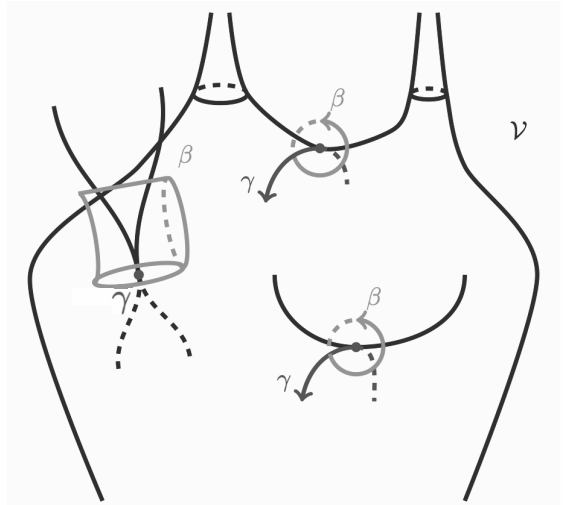

Figure 7.19 Critical points and their normal and tangential homology generators. On the right are two index-1 smooth critical points with tangential relative homology generators γ and normal homology generators $\beta \asymp S^1$. On the left is an isolated self-intersection point γ of $\mathcal{V}$, thus a zero-dimensional stratum, pictured with a two-dimensional normal link homotopy equivalent to (and in the picture homeomorphic to) a 2-torus.

where d is distance and $\boldsymbol{p}$ is a fixed point in $\mathbb{R}^n \setminus \mathcal{M}$. Explain why this is not a good Morse function to use if trying to establish the "bouquet of spheres" result for smooth varieties – described before Theorem 7.15 above – via Theorem 7.35(b).

7.4 Geometry

Theorems 7.15 and 7.35 allow us to express the Cauchy integral for coefficients as a finite sum of integrals localized near critical points (up to negligible error). Asymptotically approximating these integrals depends on the geometry of the singular set near the critical points, after which the coefficients $n_{\boldsymbol{r}}$ appearing in (7.2) must be determined. To make this process more concrete, and give an idea of its implications for coefficient asymptotics, we discuss some special cases arising often in combinatorial examples. These situations are covered in great detail in Chapters 9–11.

https://doi.org/10.1017/9781108874144.012 Published online by Cambridge University Press

Smooth points

As seen above, the quasi-local cycle $\sigma_{\boldsymbol{w}}$ corresponding to a smooth critical point $\boldsymbol{w}$ is a tube $o\gamma_{\boldsymbol{w}}$ around a $(d-1)$-chain $\gamma_{\boldsymbol{w}}$ in $\mathcal{V}_*$ such that $h_{\hat{\boldsymbol{r}}}$ is maximized on $\gamma_{\boldsymbol{w}}$ at $\boldsymbol{w}$.

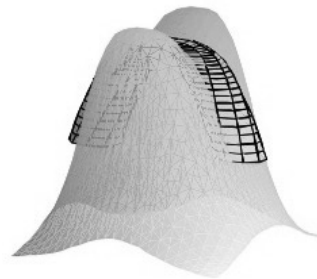

Figure 7.20 A quasi-local cycle near a smooth point.

The residue form is a complex $(d-1)$-dimensional saddle integral of the type discussed in Chapter 5. Assuming quadratic nondegeneracy, the asymptotic formula for the contribution to $a_{\boldsymbol{r}}$ from the integral over $\sigma_{\boldsymbol{w}}$ has the form

$$\Phi_{\boldsymbol{w}}(\boldsymbol{r}) = \boldsymbol{w}^{\boldsymbol{r}} \cdot |\boldsymbol{r}|^{-(d-1)/2} \cdot \left(C(\hat{\boldsymbol{r}}) + O\left(|\boldsymbol{r}|^{-1}\right)\right), \tag{7.19}$$

where $C(\hat{\boldsymbol{r}})$ is a constant arising from saddle point asymptotics and, as usual, $|\boldsymbol{r}| = |r_1| + \cdots + |r_d|$. As $\hat{\boldsymbol{r}}$ varies, the critical point $\boldsymbol{w}$ varies smoothly except for bifurcation values where $h_{\hat{\boldsymbol{r}}}$ becomes quadratically degenerate. The amplitude C also varies smoothly with $\hat{\boldsymbol{r}}$ away from bifurcation values where the topology may change, which are also points where the coefficient $n_{\boldsymbol{w}}$ in (7.2) may change. The values of $\hat{\boldsymbol{r}}$ for which $h_{\hat{\boldsymbol{r}}}$ is quadratically degenerate can be computed using the methods of Section 8.4 in Chapter 8. Removing "bad" directions partitions the set of directions into open cones over which the estimate (7.2) is uniform over compact subsets.

Transverse multiple points

When $Q(\boldsymbol{z}) = \prod_{j=1}^{k} Q_j(\boldsymbol{z})$ is a product of (potentially non-polynomial) analytic functions in a neighborhood of some $\boldsymbol{w} \in \mathbb{C}$ and the zero sets of Q_j are smooth and intersect transversely at $\boldsymbol{w}$, then we call $\boldsymbol{w}$ a *transverse multiple point*; see Figure 7.21. Note that every smooth point is trivially a transverse multiple point.

The quasi-local cycle $\sigma_{\boldsymbol{w}}$ defined by such a point $\boldsymbol{w}$ is the product of a k-torus $\beta_{\boldsymbol{w}}$ and a $(d-k)$-chain $\gamma_{\boldsymbol{w}}$. The torus $\beta_{\boldsymbol{w}}$ is a product of circles about $\boldsymbol{w}$

https://doi.org/10.1017/9781108874144.012 Published online by Cambridge University Press

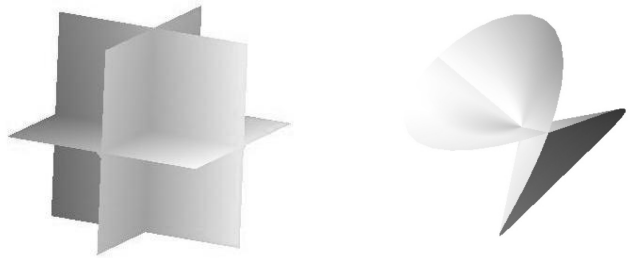

Figure 7.21 *Left:* A singular variety containing only transverse multiple points (including smooth points). *Right:* A singular variety with smooth points, a ray of (non-smooth) transverse multiple points, and a non-transverse multiple point (the origin of that ray).

in the complex normal space to each divisor Q_j. The chain $\gamma_{\boldsymbol{w}}$ is supported in the stratum defined as the common intersection of the varieties defined by the factors vanishing at $\boldsymbol{w}$, and achieves its maximum height at $\boldsymbol{w}$.

Example 7.37. If $\boldsymbol{p}$ is the common intersection of all three surfaces on the left of Figure 7.21 then $d = k = 3$ and the stratum of $\boldsymbol{p}$ is zero-dimensional. In this case $\sigma_{\boldsymbol{p}} = \beta_{\boldsymbol{p}}$ is a three torus defined by the product of circles about $\boldsymbol{p}$ in each of the three complex normal spaces to the surfaces. ◁

Example 7.38. Let $\mathcal{V}$ be the union of two complex hypersurfaces in dimension three. Any point $\boldsymbol{w}$ on the stratum S defined intersection of these two hypersurfaces is a (non-smooth) transverse multiple point. The stratum S has codimension $k = 2$ and the homology of the normal link is generated by a 2-torus $\beta_{\boldsymbol{w}}$. ◁

There is a theory of multiple residues for transverse multiple points, not too much more difficult than the residue forms already introduced, and asymptotics for an integral over a quasi-local cycle may be computed rather neatly using this approach. Such residues can be used even when the denominator is irreducible as a polynomial but locally factors into power series that converge in a neighborhood of the critical point $\boldsymbol{w}$ and each define smooth analytic varieties that intersect transversely at $\boldsymbol{w}$ (see, for instance, Example 10.4 in Chapter 10 for such a situation). The d-dimensional Cauchy integral over $\gamma_{\boldsymbol{w}} \times \beta_{\boldsymbol{w}}$ is reduced by residue computations to a $(d-k)$-dimensional integral over $\gamma_{\boldsymbol{w}}$. When $d = k$ the resulting residue integral is simply a function of $\boldsymbol{r}$, while if $k < d$ then the integral over $\gamma_{\boldsymbol{w}}$ is asymptotically approximated via the saddle point

https://doi.org/10.1017/9781108874144.012 Published online by Cambridge University Press

method. Ultimately, we typically obtain an asymptotic formula of the form

$$\Phi_{\boldsymbol{w}}(\boldsymbol{r}) = \boldsymbol{w}^{\boldsymbol{r}} \cdot |\boldsymbol{r}|^{-(d-k)/2} \cdot \left(C(\hat{\boldsymbol{r}}) + O\left(|\boldsymbol{r}|^{-1}\right)\right), \tag{7.20}$$

where again $\boldsymbol{w}$ varies smoothly with $\hat{\boldsymbol{r}}$ away from quadratic degeneracies and certain cone boundaries, and the value $\boldsymbol{w}(\hat{\boldsymbol{r}})$ is constant over a set of $\hat{\boldsymbol{r}}$ of dimension $k-1$. Since a smooth point is a special case of a transverse multiple point with $k = 1$, (7.19) is a special case of (7.20).

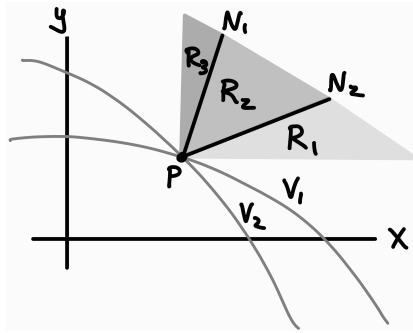

Figure 7.22 The logarithmic gradients of two transversely intersecting sheets at a critical point $\boldsymbol{p}$ decompose the first quadrant of $\mathbb{R}^2$ into three cones.

Example 7.39. Figure 7.22 illustrates two transversely intersecting smooth curves defined by the vanishing of two-dimensional functions $Q_1(x, y)$ and $Q_2(x, y)$ that meet at a single point $\boldsymbol{p}$. There are two one-dimensional strata $S_1 = \mathcal{V}(Q_1) \setminus \boldsymbol{p}$ and $S_2 = \mathcal{V}(Q_2) \setminus \boldsymbol{p}$, containing points on exactly one of the curves, together with a zero-dimensional stratum containing only $\boldsymbol{p}$. Given $\hat{\boldsymbol{r}}$ there is at most one critical point $\boldsymbol{z}_j$ on each stratum S_j, and $h_{\hat{\boldsymbol{r}}}$ is quadratically nondegenerate for any $\hat{\boldsymbol{r}}$ in the positive quadrant. As $\hat{\boldsymbol{r}}$ varies from $\boldsymbol{x} = (1, 0)$ to $\boldsymbol{y} = (0, 1)$ it crosses through two "bad" directions, given by the logarithmic gradients $N_1 = (\nabla_{\log} Q_1)(\boldsymbol{p})$ and $N_2 = (\nabla_{\log} Q_2)(\boldsymbol{p})$ shown emanating from $\boldsymbol{p}$. The zero-dimensional stratum $\boldsymbol{p}$ remains fixed, but the critical points $\boldsymbol{z}_j$ move smoothly with $\hat{\boldsymbol{r}}$ on their respective strata S_j. As $\hat{\boldsymbol{r}}$ crosses the log-normal direction N_2 the critical point $\boldsymbol{z}_2$ collides with $\boldsymbol{p}$, then when $\hat{\boldsymbol{r}}$ crosses N_1 the point $\boldsymbol{z}_1$ collides with $\boldsymbol{p}$. The positive quadrant in $\mathbb{R}^2$ can thus be broken into three regions: the cone R_1 defined by the positive real span of $\boldsymbol{x}$ and N_2, the cone R_2 defined by N_2 and N_1, and the cone R_3 defined by N_1 and $\boldsymbol{y}$. It turns out that $n_{\boldsymbol{z}_1} = n_{\boldsymbol{z}_2} = 1$ on all regions, but $n_{\boldsymbol{p}}$ is equal to one on R_2 and zero on $R_1 \cup R_3$. Accordingly, the asymptotic expansion expressed in (7.2) changes across the boundaries of these regions. ◁

https://doi.org/10.1017/9781108874144.012 Published online by Cambridge University Press

Multiple and arrangement points

When varieties intersect tangentially instead of transversely, the resulting integrals are more challenging to asymptotically approximate. However, if the intersection lattice for smooth sheets of the variety coincides with the intersection lattice for the tangent planes of these sheets then non-transversality can be handled combinatorially. Such a point is called an *arrangement point*, after hyperplane arrangements such as the one in Figure 7.23.

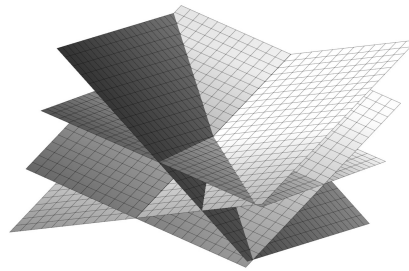

Figure 7.23 When $\mathcal{V}$ is a hyperplane arrangement, all points are arrangement points.

Exercise 7.12. For which of the polynomials $Q_1(x, y, z) = z(x-y)(x-y+z-x^2)$ and $Q_2(x, y, z) = z(x - y)(x - y + z - xyz)$ is the origin an arrangement point?

The generators $\beta_{\boldsymbol{p},j}$ for the normal link of an arrangement point are the same as for a transverse multiple point, only there are more of them.

Example 7.40. Figure 7.24 shows a case where $d = 2$ and $k = 3$. Here three one-dimensional sheets intersect pairwise transversely in a point $\boldsymbol{p}$. Instead of one two-torus $\beta_{\boldsymbol{p}}$ there are two tori $\beta_{\boldsymbol{p},1}$ and $\beta_{\boldsymbol{p},3}$, where $\beta_{\boldsymbol{p},1}$ is the product of circles about $\boldsymbol{p}$ in $\mathcal{V}_2$ and $\mathcal{V}_3$, and $\beta_{\boldsymbol{p},3}$ is the product of circles about $\boldsymbol{p}$ in $\mathcal{V}_1$ and $\mathcal{V}_2$. One might have expected a third torus $\beta_{\boldsymbol{p},2}$, a product of circles about $\boldsymbol{p}$ in $\mathcal{V}_1$ and $\mathcal{V}_3$, and indeed there is such a torus, however this final torus is not linearly independent of the first two because $\beta_{\boldsymbol{p},1} - \beta_{\boldsymbol{p},2} + \beta_{\boldsymbol{p},3} = 0$ in the relevant homology class. ◁

A similar multivariate residue computation as in (7.20) leads to a formula of the form

$$\Phi_{\boldsymbol{w}}(\boldsymbol{r}) = \boldsymbol{w}^{\boldsymbol{r}} \cdot |\boldsymbol{r}|^{-(d-k)/2} \cdot \left(P_{\boldsymbol{r}}(\boldsymbol{w}) + O\left(|\boldsymbol{r}|^{-1}\right)\right), \tag{7.21}$$

where $P_{\boldsymbol{r}}(\boldsymbol{w})$ is a polynomial of degree at most $m - k$ with m the number of sheets intersecting at $\boldsymbol{w}$ and k the codimension of the stratum containing

https://doi.org/10.1017/9781108874144.012 Published online by Cambridge University Press

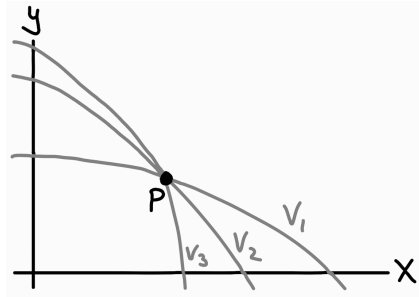

Figure 7.24 Quasi-local cycles at an arrangement point with $d = k = 2$.

$\boldsymbol{w}$. This approach also works when Q has repeated factors, provided that m is counted with the right multiplicity. Further details are given in Chapter 10.

Cone points

Beyond the above cases are critical points near which $\mathcal{V}$ does not look like a union of smooth sheets. We give a general analysis only in one case, namely when $\mathcal{V}$ is locally diffeomorphic to a cone $\sum_{j=1}^{d} z_j^2 = 0$. Such an isolated singularity is called a ***cone point singularity***, and is illustrated in Figure 7.25. Cone points arise, among other places, in statistical physics.

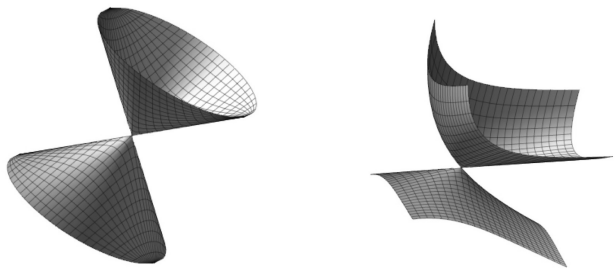

Figure 7.25 Two examples of cone point singularities.

Chapter 11 is devoted to the analysis of cone-point singularities. For any isolated singularity $\boldsymbol{w}$ we have $d = k$, so the stratum containing $\boldsymbol{w}$ is zero-dimensional, the cycle $\gamma_{\boldsymbol{w}}$ is just a point, and $\sigma_{\boldsymbol{w}} = \beta_{\boldsymbol{w}}$. General theory derived in [ABG70] indicates what to expect for the leading asymptotic term of $\int_{\beta_{\boldsymbol{w}}} \boldsymbol{z}^{-\boldsymbol{r}-\mathbf{1}} P(\boldsymbol{z})/Q(\boldsymbol{z})\, d\boldsymbol{z}$ at an isolated singularity $\boldsymbol{w}$: it is given by the inverse Fourier transform of the reciprocal of the leading homogeneous term of Q near

https://doi.org/10.1017/9781108874144.012 Published online by Cambridge University Press

$\boldsymbol{w}$. For a cone point, the inverse Fourier transform yields an asymptotic contribution

$$\Phi_{\boldsymbol{w}}(\boldsymbol{r}) = C(\boldsymbol{w}) \cdot \tilde{q}(\boldsymbol{r})^{1-d/2} \cdot \left(1 + O\left(|\boldsymbol{r}|^{-1}\right)\right), \tag{7.22}$$

where $\tilde{q}$ is the dual quadratic form in $\boldsymbol{r}$-space to the quadratic leading term of Q at $\boldsymbol{w}$.

Example 7.41. The so-called ***cube grove*** creation generating function, analyzed in Example 11.43 of Chapter 11, is the rational function

$$F(x, y, z) = \frac{1}{1 + xyz - (1/3)(x + y + z + xy + xz + yz)}. \tag{7.23}$$

The variety $\mathcal{V}$ is smooth except at the single point $(1, 1, 1)$ where, after an orthogonal affine change of variables and a translation of the origin to $(1, 1, 1)$, the denominator of F looks asymptotically like the quadratic cone $2xy + 2xz + 2yz = 0$. The asymptotic formula given in Corollary 11.44 implies

$$a_{rst} \sim \frac{1}{\pi}\left[rs + rt + st - \frac{1}{2}(r^2 + s^2 + t^2)\right]^{-1/2}$$

when (r, s, t) lies inside the dual to the tangent cone to the denominator of F. ◁

For more general isolated singularities, analysis via inverse Fourier transforms lead to asymptotic contributions of the form

$$\Phi_{\boldsymbol{w}}(\boldsymbol{r}) = \boldsymbol{w}^{\boldsymbol{r}} \cdot |\boldsymbol{r}|^{-d-\kappa} \cdot \left(C(\hat{\boldsymbol{r}}) + O\left(|\boldsymbol{r}|^{-1}\right)\right), \tag{7.24}$$

which are valid as $\hat{\boldsymbol{r}}$ varies over the open dual cone to the tangent cone to $\mathcal{V}$ at $\boldsymbol{w}$, and uniform if $\hat{\boldsymbol{r}}$ is restricted to any compact subcone. The constant κ is the homogeneous degree of F at $\boldsymbol{w}$.

Exercise 7.13. Give a simple reason why cone points can never be multiple points.

Examples from the literature of these further variants include isolated singularities where Q is locally homogeneous of degree three [KP16] or four [BP21], or where $\mathcal{V}$ is the union of a quadratic cone with a smooth sheet passing through the cone point [BP11].

The first two of these examples are illustrated in Figure 7.26. Figure 7.27 shows the final example, where $\mathcal{V}$ is locally the union of a quadratic cone and a smooth sheet; an asymptotic formula is derived in [BP11]. In general asymptotics for this sort of geometry would be expressed in terms of an elliptic

https://doi.org/10.1017/9781108874144.012 Published online by Cambridge University Press

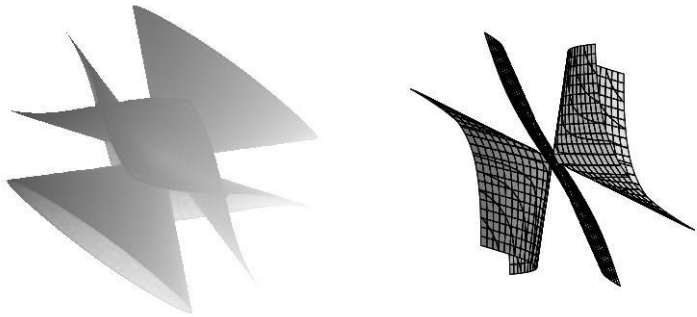

Figure 7.26 Isolated singularities of degree greater than 2.

integral, but in this case there is an explicit formula (see Theorem 11.49)

$$a_{rst} \sim \frac{1}{\pi} \arctan\left(\frac{\sqrt{1 - 2\hat{r}^2 - 2\hat{s}^2}}{1 - 2\hat{s}} \right).$$

A plot of this limiting behavior against $\hat{r}$ is shown on the right side of Figure 7.27.

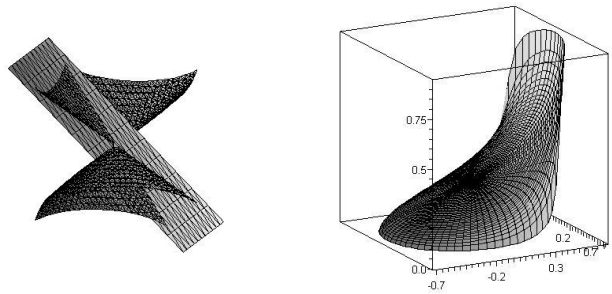

Figure 7.27 *Left:* A singular set consisting of a cone and a smooth sheet. *Right:* Asymptotic behavior of the corresponding coefficient sequence.

Exercise 7.14. Which of the two graphs in Figure 7.26 have arrangement points that are not smooth points?

https://doi.org/10.1017/9781108874144.012 Published online by Cambridge University Press

7.5 Deformations

Finally, we end this chapter with a treatment of critical points and critical values at infinity. After giving a rigorous definition of such points we show how, in their absence, to construct the deformations that prove Lemmas 7.25 and 7.28. These two lemmas then imply Theorems 7.15 and 7.30.

7.5.1 Critical points at infinity

As described above and in Appendix C, the results of Morse theory typically require a *proper* height function so that certain gradient flows are guaranteed to reach points of low height, except when they get stuck near critical points. This properness condition is often satisfied in classical contexts by studying compact spaces, however our singular varieties are not compact and we often have non-proper height functions.

Our goal, therefore, is to formulate weaker but still sufficient conditions for there to be no topological obstructions to deforming our Cauchy integral to points of low height, proving results like Lemma 7.14 and Theorem 7.35 above. A considerable stream of topological research has gone into defining *bifurcation values*, at which the height function is not a locally trivial fibration and the topology of the space changes. While exact conditions for these topological obstructions remain murky, we care only about pushing down domains of integration to lower height, and may thus proceed by generalizing our definition of critical points (and critical values) to include "points at infinity."

We begin by defining the binary relation $\mathcal{R} \subseteq \mathbb{C}^d_* \times \mathbb{CP}^{d-1}$ that holds for a pair $(\boldsymbol{z}, \hat{\boldsymbol{r}})$ when the differential $dh_{\hat{\boldsymbol{r}}}|_S$ of the height function $h_{\hat{\boldsymbol{r}}}$ restricted to the stratum S containing $\boldsymbol{z}$ vanishes at $\boldsymbol{z}$. To facilitate computation we view $\hat{\boldsymbol{r}}$ as an element of $\mathbb{CP}^{d-1}$.

Definition 7.42 (CPAI)**.** Let $\overline{\mathcal{R}}$ be the closure in $\mathbb{CP}^d \times \mathbb{CP}^{d-1}$ of the relation $\mathcal{R}$. A ***critical point at infinity*** (CPAI) in the direction $\hat{\boldsymbol{r}}_*$ is a limit point $(\boldsymbol{z}_*, \hat{\boldsymbol{r}}_*)$ in $\overline{\mathcal{R}}$ of points $(\boldsymbol{z}, \hat{\boldsymbol{r}}) \in \mathcal{R}$ such that $\boldsymbol{z}_* \notin \mathbb{C}^d_*$. When necessary we refer to our usual notion of critical points (not at infinity) as ***affine critical points*** to distinguish them from critical points at infinity.

In other words, a critical point at infinity in the direction $\hat{\boldsymbol{r}}_*$ is a limit, lying either at infinity or on a coordinate plane, of a sequence $\boldsymbol{z}^{(k)}$ of critical points contained in strata S_k such that the projection of $\hat{\boldsymbol{r}}_*$ to the tangent space of N_k at $\boldsymbol{z}^{(k)}$ converges to zero as $k \to \infty$ (i.e., $\hat{\boldsymbol{r}}_*$ lies in the "limit normal space" of the sequence $\boldsymbol{z}^{(k)}$) – see Figure 7.28.

To track the heights of CPAIs, given $\hat{\boldsymbol{r}} \in \mathbb{CP}^{d-1}$ we define the ternary relation

https://doi.org/10.1017/9781108874144.012 Published online by Cambridge University Press

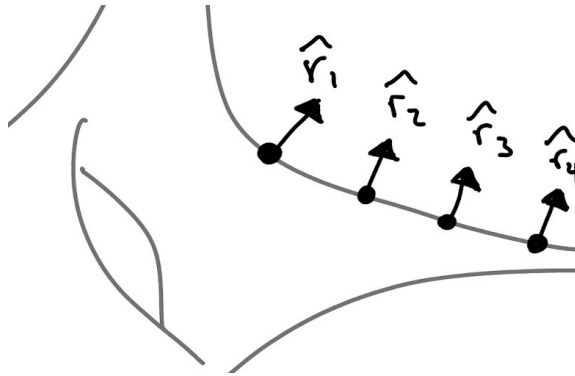

Figure 7.28 A sequence of points moving out to infinity, such that the logarithmic gradient of Q approaches the vector v pointing straight up. This sequence witnesses a critical point at infinity in the direction v.

$\mathcal{T}(\hat{r}) \subseteq \mathbb{C}^d_* \times \mathbb{CP}^{d-1} \times \mathbb{R}$ containing elements (z, y, η) such that $(z, y) \in \mathcal{R}$ and $h_{\hat{r}}(z) = \eta$.

Definition 7.43 (CVAI)**.** Let $\overline{\mathcal{T}} \subseteq \mathbb{CP}^d \times \mathbb{CP}^{d-1} \times \mathbb{R}$ be the closure of the ternary relation $\mathcal{T}$ in $\mathbb{CP}^d \times \mathbb{CP}^{d-1} \times \mathbb{R}$. We call η a ***critical value at infinity*** *(*CVAI*)* if some point $(z_*, \hat{r}_*, \eta)$ is in $\overline{\mathcal{T}}$ and $z_* \notin \mathbb{C}^d_*$.

7.5.2 Vector fields and flows

The results we prove in this section are based on [BMP22, Theorem 1].

Theorem 7.44 (homotopy equivalences in the absence of CVAI)**.** *Fix a direction $\hat{r}$ and a Whitney stratification $\{S_\alpha : \alpha \in I\}$ of $(\mathbb{C}^d_*, \mathcal{M})$.*

(i) If there are neither affine critical values nor CVAI in the interval $[a, b]$ then the inclusion of $\mathcal{M}_{\leq a}$ into $\mathcal{M}_{\leq b}$ is a homotopy equivalence. The same is true replacing $\mathcal{M}$ by any stratum S of $\mathcal{V}_*$.

(ii) If there are no CVAI in $[a, b]$ but there is a single affine critical value $c \in [a, b]$ and it corresponds to the set of critical points $z_1, \ldots, z_m$ then there is a stratified flow deforming any chain C in $\mathcal{M}$ down to a chain in the union of $M_{<c}$ with sufficiently small balls about each z_i. When $[c - \varepsilon, c + \varepsilon] \subseteq (a, b)$, this induces a homotopy equivalence between $(\mathcal{M}_{c+\varepsilon}, \mathcal{M}_{c-\varepsilon})$ and the direct sum of attachment spaces $\mathcal{M}^{z,loc}$ defined in Section 7.3 above (see also Definition C.31 and Figure C.6 in Appendix C).

The first part of Theorem 7.44 directly implies Lemma 7.25. The main work

https://doi.org/10.1017/9781108874144.012 Published online by Cambridge University Press

in proving Theorem 7.44 comes from establishing the following result, which requires bounding elements of a vector field. Although general stratified spaces do not come equipped with Riemannian metrics, we deal only with spaces embedded in $\mathbb{C}^d \cong \mathbb{R}^{2d}$ and the norm of any vector or covector refers to the norm inherited from this embedding.

Lemma 7.45 ([BMP22, Lemma 2])**.** *Suppose $a < b$ are real numbers such that $h_{\hat{\boldsymbol{r}}}$ has no* CVAI *in the interval $[a, b]$ and one affine critical value in $c \in [a, b]$, not at either endpoint. Then there is a vector field $\boldsymbol{v}$ on $\mathbb{C}^d_* \cap h^{-1}_{\hat{\boldsymbol{r}}}[a, b]$ with the following properties.*

(i) $\boldsymbol{v}$ *is smooth on strata and continuous on $\mathbb{C}^d_*$;*
(ii) $\boldsymbol{v}$ *is tangent to strata;*
(iii) $\boldsymbol{v}$ *is a controlled vector field in the sense of [Mat70, Section 9];*
(iv) $\boldsymbol{v}$ *is bounded;*
(v) $\boldsymbol{v}$ *has unit downward speed, meaning $dh_{\hat{\boldsymbol{r}}}(\boldsymbol{v}) \equiv -1$.*

The first, relatively easy, step in establishing Lemma 7.45 is to show that $|dh_{\hat{\boldsymbol{r}}}|$ is bounded away from zero except near critical points.

Lemma 7.46 ([BMP22, Lemma 1])**.** *Suppose h is a Morse function on a stratified space $\mathcal{V}_* \subseteq \mathbb{C}^d_*$, with no* CVAI *in $[a, b]$. Then, excluding an arbitrarily small neighborhood $\mathcal{N}$ of critical points, the differential dh has its magnitude bounded away from zero, meaning $|dh| \geq \delta(\mathcal{N}) > 0$.*

Proof It suffices to prove the result when dh is restricted to an arbitrary stratum S. Let $S_{[a,b]}$ denote the elements of S with height in $[a, b]$ and let $\mathcal{L} = \mathbb{R}^d \times (\mathbb{R}/2\pi\mathbb{R})^d$ denote the logarithmic parametrizing space for $\mathbb{C}^d_*$ via the exponential map $\exp : \mathcal{L} \to \mathbb{C}^d_*$. In this parametrization, $h_{\hat{\boldsymbol{r}}}$ becomes $\tilde{h} = h_{\hat{\boldsymbol{r}}} \circ \exp$. This parametrization is useful because $d\tilde{h}$ is the constant vector $\hat{\boldsymbol{r}}$ (formally, $d\tilde{h} = \sum_{j=1}^d r_j dx_j + 0 dy_j$ is a constant with respect to the embedding in $\mathcal{L}$ obtained from the embedding in $\mathbb{C}^d_*$, pulled back via exp). We use tildes to denote inverse images under this parametrization, meaning $\widetilde{\texttt{critical}} = \exp^{-1}[\texttt{critical}]$ is the inverse image of the set of critical points of the Morse function h.

Assume towards a contradiction that the norm of the tangential differential is *not* bounded from below on $\widetilde{S}_{[a,b]} \setminus \mathcal{N}$, where $\mathcal{N}$ is a neighborhood of $\widetilde{\texttt{critical}}$ in $\mathcal{L}$, and let $\tilde{\boldsymbol{x}}_k$ be a sequence in $\widetilde{S}_{[a,b]} \setminus \mathcal{N}$ for which $|d\tilde{h}_{\widetilde{S}}(\tilde{\boldsymbol{x}}_k)|$ goes to zero. This sequence has no limit points whose height lies outside of $[a, b]$ and no limit points in $\widetilde{\texttt{critical}}_{[a,b]}$. There are also no affine limit points outside of $\widetilde{\texttt{critical}}$, because if $\boldsymbol{x} \to \boldsymbol{y}$ with $\boldsymbol{y}$ in a substratum $\widetilde{S}_y$ then $|d\tilde{h}_{\widetilde{S}_y}(\boldsymbol{y})| \leq \liminf_{\boldsymbol{x}\to\boldsymbol{y}} |d\tilde{h}_{\widetilde{S}}(\boldsymbol{x})|$ since the projection of the differential onto a substratum is

https://doi.org/10.1017/9781108874144.012 Published online by Cambridge University Press

at most the projection onto $\widetilde{S}$. By compactness, $\{\boldsymbol{x}_k\}$ must have a limit point $\boldsymbol{x} \in \mathbb{CP}^d$. It follows from ruling out noncritical points, and affine stationary points with heights inside or outside of $[a, b]$, that $\boldsymbol{x}$ lies at infinity. The sequence therefore defines a CPAI of height c, contradicting the hypothesis and proving the lemma. □

With Lemma 7.46 in hand, we outline the proof of Lemma 7.45 before returning to Theorem 7.44.

Sketch of proof of Lemma 7.45 This lemma for proper height functions is the usual Morse theoretic construction of stratified gradient-like vector fields, as found in standard references [GM88; ABG70]. It is proved by using a partition of unity to piece together the unit-speed downward gradient of $h_{\hat{\boldsymbol{r}}}$ restricted to each stratum and then extended to a neighborhood of the stratum in $\mathbb{C}^d_*$ via the local product structure. Property (v), unit downward speed, then follows from Lemma 7.46. In the nonproper case, the biggest headache is extending to the product; this was the motivation for the notion of *control data*, developed in [Mat70]. When $h_{\hat{\boldsymbol{r}}}$ is not proper, there is no *a priori* guarantee that the descent rate divided by the magnitude of the vector remains bounded away from zero, even locally. This is because the Whitney condition fits these C^∞ strata in a way that is in principle only C^0. In fact, Mather's argument contains the seeds of a proof for this fact, which is accomplished via some linear algebra and further explicit use of the Whitney conditions. See [BMP22, Lemma 2] for full details. □

Proof of Theorem 7.44 Let $\boldsymbol{v}$ be the vector field constructed in Lemma 7.45, altered so as to be zero on $\mathcal{M}_{\leq a}$. This vector field defines a flow $\Phi(x, t)$ such that

- $\dfrac{d}{dt}\Phi(x, t) = \boldsymbol{v}(x)$ when $h_{\hat{\boldsymbol{r}}}(x) \in (a, b]$;
- $\Phi(x, t)$ is defined for $0 \leq t \leq h_{\hat{\boldsymbol{r}}}(x) - a$ and, for t in this range, $h_{\hat{\boldsymbol{r}}}(\Phi(x, t)) = h_{\hat{\boldsymbol{r}}}(x) - t$;
- the map $\psi(x) = \Phi(x, b - a)$ is a continuous map on $\mathcal{M}_{\leq b}$ with range $\mathcal{M}_{\leq a}$ and fixing $\mathcal{M}_{\leq a}$.

It follows from these properties that the inclusion $\iota : \mathcal{M}_{\leq a} \to \mathcal{M}_{\leq b}$ is a homotopy equivalence: $\psi \circ \iota$ is the identity map on $\mathcal{M}_{\leq a}$ while $\iota \circ \psi$ is homotopic to the identity map on $\mathcal{M}_{\leq b}$ via the homotopy Φ on $\mathcal{M}_{\leq b} \times [0, b - a]$. This is sufficient to imply conclusion (i) of Theorem 7.44, and also proves the weaker version of (ii) found in [BMP22], namely that any cycle in $\mathcal{M}_{\leq b}$ may be deformed to lie in the union of $\mathcal{M}_{\leq c-\varepsilon}$ with arbitrarily small neighborhoods of

https://doi.org/10.1017/9781108874144.012 Published online by Cambridge University Press

each critical point. However, this argument does not imply that the deformation is induced by a homotopy equivalence.

To that end, let $\kappa(\boldsymbol{x}) = \min\{|\boldsymbol{x} - \boldsymbol{z}| : \boldsymbol{z} \in \texttt{critical}\}$ denote distance to the critical set. For $s > 0$, define a new vector field $\boldsymbol{v}_s$ by

$$\boldsymbol{v}_s(\boldsymbol{x}) = \begin{cases} \boldsymbol{v}(\boldsymbol{x}) & \kappa(\boldsymbol{x}) \geq s \\ \rho(\kappa(\boldsymbol{x}))\boldsymbol{v}(\boldsymbol{x}) & \kappa(\boldsymbol{x}) \in [s/2, s] \\ 0 & \kappa(\boldsymbol{x}) \leq s/2 \end{cases},$$

where ρ is a smooth nondecreasing function with $\rho(s/2) = 0$ and $\kappa(s) = 1$.

Fix $\varepsilon > 0$ with $[c - \varepsilon, c + \varepsilon] \subseteq (a, b)$ and let $\Phi_s(x, t)$ denote the flow defined similarly to Φ but with $\boldsymbol{v}_s$ in place of $\boldsymbol{v}$. Let $\tau(\boldsymbol{x}) = \Phi_s(\boldsymbol{x}, 2\varepsilon)$ denote the time 2ε map for the flow Φ_s. Because $h = h_{\hat{\boldsymbol{r}}}$ is nonincreasing along Φ_s, points in $\mathcal{M}_{\leq c-\varepsilon}$ remain inside $\mathcal{M}_{\leq c-\varepsilon}$, hence the flow defines a homotopy equivalence between the pairs $(\mathcal{M}_{c+\varepsilon}, \mathcal{M}_{c-\varepsilon})$ and $(X, \mathcal{M}_{c-\varepsilon})$, where $X = \tau[\mathcal{M}_{c+\varepsilon}]$.

Define a modified height function $g = h \circ \tau$. We claim that g has the same critical points as h in $h^{-1}([c-\varepsilon, c+\varepsilon])$. To see this, first observe that trajectories of Φ_s are either rest trajectories at points in the set $V_0 = \{\boldsymbol{x} : \boldsymbol{v}_s(\boldsymbol{x}) = 0\}$ or else never enter V_0. Indeed, this follows from the fact that $\boldsymbol{v}_s$ is tangent to all strata, smooth on every stratum, and that trajectories of a flow defined by a smooth vector field cannot merge. Inside V_0, the height functions h and g are equal, and hence have the same critical points. Outside V_0, the differential $dg|_S$ can never vanish because $dg|_S(\boldsymbol{v}) < 0$; this follows from the fact that for $\boldsymbol{v} \in S$, the map $dg(\boldsymbol{v})(\boldsymbol{x}) = d(h \circ \tau)(\boldsymbol{v})(\boldsymbol{x})$ sends $\boldsymbol{v}$ to $dh(D\tau(\boldsymbol{v}))$. On trajectories, the map $D\tau$ carries $\boldsymbol{v}_s \in T_{\boldsymbol{x}}(S)$ to $\rho(\tau(\boldsymbol{x})) \in T_{\tau(\boldsymbol{x})}(S)$, where $\rho(\tau(\boldsymbol{x})) > 0$. Thus

$$dg(\boldsymbol{v}_s)(\boldsymbol{x}) = \rho(\tau(\boldsymbol{x}))dh(\boldsymbol{v}_s)(\tau(\boldsymbol{x})) = -\rho(\tau(\boldsymbol{x})) < 0\,,$$

showing that $dg|_S$ is nonvanishing outside V_0 and proving the claim.

The map τ takes all points of $\mathcal{M}_{\leq c+\varepsilon}$ into $\mathcal{M}_{\leq c-\varepsilon}$, except possibly for those whose trajectories come within distance s of the critical set within time 2ε. Because $\boldsymbol{v}$ is bounded, trajectories coming within s of the (finite) critical set within time 2ε are all contained in some compact set K, independent of $s \in [0, 1]$. Therefore, the difference $X \setminus \mathcal{M}_{c-\varepsilon}$ is bounded and g is a proper height function on the pair $(X, \mathcal{M}_{c-\varepsilon})$, in the sense that the inverse image of a compact set in $X \setminus \mathcal{M}_{c-\varepsilon}$ is compact.

We may now apply the results of stratified Morse theory (see Theorem D.21 in Appendix D). The result is that the pair $(X, \mathcal{M}_{\leq c-\varepsilon})$ is homotopy equivalent to the direct sum of pairs $(\mathcal{N}(\boldsymbol{z}) \cup \mathcal{M}_{c-\delta}, \mathcal{M}_{c-\delta})$ as $\boldsymbol{z}$ varies over the critical points of height c and $\mathcal{N}(\boldsymbol{z})$ can be chosen to be arbitrarily small neighborhoods of these, after which δ is chosen sufficiently small. We have seen, in

https://doi.org/10.1017/9781108874144.012 Published online by Cambridge University Press

addition, that each cycle in X may be deformed into the union of $\mathcal{M}_{c-\delta}$ and the neighborhoods $\mathcal{N}(\boldsymbol{z})$ by running the flow $\boldsymbol{v}_s$, hence the homotopy equivalence is induced by this flow. Finally, having shown that the flow induces a homotopy equivalence between $(\mathcal{M}_{c+\varepsilon}, \mathcal{M}_{c-\varepsilon})$ and $(X, \mathcal{M}_{c-\varepsilon})$, we can pick s sufficiently small and $\mathcal{N}(\boldsymbol{z})$ and δ so that $\delta < \varepsilon$, finishing the proof of part (*ii*). □

Notes

The rigorous foundation of the main theorems of this book in the framework of Morse theory is new to the second edition. Before the appearance of [BMP22], Morse-theoretic results were not available because $h_{\hat{\boldsymbol{r}}}$ is not, in general, a proper function. Therefore, in the first edition, Morse theory was used only as a motivation and individual results were obtained via hands-on deformations and surgeries, informed by Morse theory but proved as special cases, tailored to the individual hypotheses.

Asymptotic formulae in the presence of smooth strictly minimal points first appeared in [PW02], followed by formulae for strictly minimal multiple points in [PW04]. Results proving the irrelevance of non-critical minimal points were derived in [Bar+10], and then in greater generality in [BP11], with an overview presented in [Pem10]. The proof sketch of Lemma 7.6 was suggested to us by Tony Pantev.

The second part of Theorem 7.44 is an improvement on the result originally published in [BMP22]. There, it was shown that cycles may be pushed down into the union of levels below the critical value and neighborhoods of the critical points, but not that this union is homotopy equivalent to the space at a level above the critical value. The sticking point is that the latter requires a deformation remaining at all times within the union, which requires geometric facts developed at length throughout [GM88]. The present proof avoids this by using the results of [BMP22] to eliminate escape to infinity, then finishing by using results of [GM88] as a black box.

Additional exercises

Exercise 7.15. When $d = 2$, the map $\mathrm{Relog} : \mathcal{V}_* \to \mathbb{R}^d$ is locally one-to-one at most points. We say that $\mathtt{amoeba}(f)$ is a *doublet* if $\mathrm{Relog}^{-1}(\boldsymbol{x})$ has cardinality precisely 2 for all $\boldsymbol{x}$ in the interior of $\mathtt{amoeba}(f)$. Give a proof by picture that if $\mathtt{amoeba}(f)$ is a doublet then there is a natural isomorphism κ between the reduced homology group $\tilde{H}_0(\mathtt{amoeba}(f)^c)$ and $H_1(\mathcal{V}_*)$, defined by $\kappa([\boldsymbol{x}'] - [\boldsymbol{x}]) = \mathbf{INT}(\mathbf{T}(\boldsymbol{x}), \mathbf{T}(\boldsymbol{x}'))$.

https://doi.org/10.1017/9781108874144.012 Published online by Cambridge University Press

Exercise 7.16. Let $Q(x,y) = 5 - x - x^{-1} - y - y^{-1}$ and $F(x,y) = 1/Q(x,y)$.

(a) Sketch $\texttt{amoeba}(Q)$ and mark a point in each component of $\texttt{amoeba}(Q)^c$.

(b) Recall that the *Fourier series* of F is the series $\hat{F}(x,y) = \sum_{a,b\in\mathbb{Z}} c_{a,b} e^{i(ax+by)}$, where

$$c_{a,b} = \frac{1}{(2\pi)^2} \int_{-\pi}^{\pi} \int_{-\pi}^{\pi} F(x,y) e^{-in(ax+by)} dxdy.$$

The Fourier series $\hat{F}$ is related to the Laurent expansion of F corresponding to one component of $\texttt{amoeba}(f)^c$. Identify this component, and describe the relation.

(c) Prove that $\texttt{amoeba}(Q)$ is a doublet.

(d) Let $\boldsymbol{x} = (0,0)$ and $\boldsymbol{x}' = (0,2)$. Show that $\boldsymbol{x}$ and $\boldsymbol{x}'$ are in different components of the complement of $\texttt{amoeba}(Q)$, and describe or sketch $\mathbf{INT}(\mathbf{T}(\boldsymbol{x}), \mathbf{T}(\boldsymbol{x}'))$.

(e) Find all critical points of $\mathcal{V}_*$ in the direction $\boldsymbol{r} = (1/3, 2/3)$ and mark them on your sketch from part (*a*).

(f) Deform the intersection cycle γ you found in part (*d*) until its highest and lowest points are critical points in direction $\boldsymbol{r} = (1/3, 2/3)$. At which of these points is the phase $h_{\hat{\boldsymbol{r}}}$ maximized on γ?

(g) What does your result tell you about the coefficients of the Fourier series for F?

Exercise 7.17. For $Q(x,y,z) = z(x-y)(x-y+z-xyz)$, as in Exercise 7.12, state the dimension of the stratum containing the origin, describe the normal link, and describe the local homology group $H_3(\mathcal{M}^{\boldsymbol{p},\mathrm{loc}})$ when $\boldsymbol{p}$ is the origin and $\boldsymbol{r}$ is a direction of your choice (as usual, $\mathcal{M} = \mathbb{C}_*^d \setminus \mathcal{V}_Q$).

https://doi.org/10.1017/9781108874144.012 Published online by Cambridge University Press